

Aus dem Zentrum für Augenheilkunde der Universität zu Köln
Klinik und Poliklinik für Allgemeine Augenheilkunde
Direktor: Universitätsprofessor Dr. med. C. Cursiefen

***Rbpms* is essential for the specification of retinal ganglion cell identity**

Inaugural-Dissertation zur Erlangung der Doktorwürde
der Medizinischen Fakultät
der Universität zu Köln

vorgelegt von
Panpan Li
aus Nei Mongol, China

promoviert am 06. Februar 2025

Gedruckt mit Genehmigung der Medizinischen Fakultät der Universität zu Köln
2025

Dekan: Universitätsprofessor Dr. med. G. R. Fink

1. Gutachterin: Universitätsprofessorin Dr. med. V. Prokosch
2. Gutachterin: Universitätsprofessorin Dr. med. Dr. nat. med. M. A. Rüger

Erklärung

Ich erkläre hiermit, dass ich die vorliegende Dissertationsschrift ohne unzulässige Hilfe Dritter und ohne Benutzung anderer als der angegebenen Hilfsmittel angefertigt habe; die aus fremden Quellen direkt oder indirekt übernommenen Gedanken sind als solche kenntlich gemacht.

Bei der Auswahl und Auswertung des Materials sowie bei der Herstellung des Manuskriptes habe ich Unterstützungsleistungen von folgenden Personen erhalten:

Universitätsprofessorin Dr. med. Verena Prokosch, Universitätsprofessor PhD Leo Kurian, PhD Hisham Bazzi, Dr. med. Hanhan Liu, Herrn Xin Shi, Frau Rodica-Aurelia Maniu, Frau Lisa Wirtz und Frau Pia Richter.

Weitere Personen waren an der Erstellung der vorliegenden Arbeit nicht beteiligt. Insbesondere habe ich nicht die Hilfe einer Promotionsberaterin/eines Promotionsberaters in Anspruch genommen. Dritte haben von mir weder unmittelbar noch mittelbar geldwerte Leistungen für Arbeiten erhalten, die im Zusammenhang mit dem Inhalt der vorgelegten Dissertationsschrift stehen.

Die Dissertationsschrift wurde von mir bisher weder im Inland noch im Ausland in gleicher oder ähnlicher Form einer anderen Prüfungsbehörde vorgelegt.

Die in dieser Arbeit angegebenen Experimente sind nach entsprechender Anleitung durch Universitätsprofessor Dr. med. Verena Prokosch, Universitätsprofessorin PhD Leo Kurian und PhD Hisham Bazzi von mir selbst ausgeführt worden.

Die dieser Arbeit zugrunde liegenden Experimente sind von mir mit Unterstützung von Dr. med. Hanhan Liu und Herrn Xin Shi und Frau Lisa Wirtz und dem technischen Assistenten Frau Rodica-Aurelia Maniu und Frau Pia Richter durchgeführt worden.

Erklärung zur guten wissenschaftlichen Praxis:

Ich erkläre hiermit, dass ich die Ordnung zur Sicherung guter wissenschaftlicher Praxis und zum Umgang mit wissenschaftlichem Fehlverhalten (Amtliche Mitteilung der Universität zu Köln AM 132/2020) der Universität zu Köln gelesen habe und verpflichte mich hiermit, die dort genannten Vorgaben bei allen wissenschaftlichen Tätigkeiten zu beachten und umzusetzen.

Köln, 29.04.2024

Unterschrift:

ACKNOWLEDGEMENTS

At this special juncture, I am filled with profound gratitude and wish to extend my deepest thanks to each individual who has offered their unwavering support throughout writing and editing this thesis.

First and foremost, my heartfelt appreciation goes to my advisor, Prof. Dr. Verena Prokosch. She not only gave me the invaluable opportunity to explore this topic but also undertook the scientific supervision of this work. Her extensive support throughout the implementation and execution of the research is beyond what words can express. I am sincerely grateful for everything.

My thanks also go to Prof. Dr. Leo Kurain for our numerous in-depth discussions and for his constructive feedback and critique, which I have found immensely valuable. Additionally, I am sincerely thankful to Dr. Hisham Bazzi and his colleagues, Ms. Lisa Wirtz and Ms. Pia Richter, for their cooperation and support in providing embryonic tissue, which was crucial for the realization of this project.

I am also grateful to Dr. Hanhan Liu, Mr. Xin Shi, and Ms. Rodica-Aurelia Maniu for their generous assistance in this study. Their collaborative participation was vital to the implementation of the project.

I extend my heartfelt thanks to all the current and former members of our research group. Dr. Maoren Wang, Yuan Feng, Layla Fruehn, Dr. Jennifer Kern, Sylvi El Agha, Xiaosha Wang, Dr. Julia Prinz, and Tienan Qi, their support, the pleasant working atmosphere, and the spirit of collaboration made this work much more smooth and enjoyable.

Lastly, I give special thanks to my parents and family for their consistent encouragement and support in pursuing my dreams. Their unwavering encouragement and support have provided endless motivation and confidence to chase my aspirations. The positive energy I received on my journey stems from their love and perseverance, making me more resolute and courageous.

Dedication
To my beloved family

TABLE OF CONTENTS

ABBREVIATION	7
1. DEUTSCHE ZUSAMMENFASSUNG	9
2. SUMMARY	10
3. INTRODUCTION	11
3.1. RBPMS expression in the retina of mammals and non-mammals	11
3.2. RBPMS has the potential to regulate the development of RGCs in the retina of vertebrates.	11
3.3. RBPMS could act as a marker for RGC degeneration	13
3.4. Glaucoma	14
4. MATERIALS AND METHODS	15
4.1. Animals Used in Experiments	15
4.2. Aging mice	15
4.3. Preparation of retinal explants	15
4.4. Elevated Hydrostatic Pressure Model	16
4.5. Oxidative Stress Model	16
4.6. Generation and genotyping of <i>Rbpms</i> mutant mice	16
4.7. Immunohistochemistry	17
4.7.1. Tissue preparation	17
4.7.2. Histopathological analysis of embryonic retinas	17
4.7.3. Retinal flat mount RGC quantification	17
4.7.4. Immunofluorescence labeling in Embryo or Adult Retinal cryosections	18
4.8. Analysis of Statistical Data	19
5. RESULTS	20

5.1.	Variation of RBPMS in response to aging	20
5.2.	RBPMS loss in retinal neurodegenerative diseases	22
5.2.1.	RBPMS expression decreases under elevated hydrostatic pressure	22
5.2.2.	RBPMS expression declines under oxidative stress	24
5.3.	Characteristics and Spatial Distribution of Structural Features of Rbpms in Age-Related Retinal Neurodegeneration	26
5.4.	RBPMS expression in the GCL of the embryonic retina	28
5.5.	<i>Rbpms</i> deletion causes delayed development of embryonic retinal lamination patterns.	30
5.6.	<i>Rbpms</i> mutant retina RGC differentiation is significantly impeded.	31
5.7.	RGCs fate specification is perturbed in the absence of <i>Rbpms</i> .	34
6.	DISCUSSION	37
6.1.	Conclusion	43
6.2.	Limitations of the project	43
7.	REFERENCES	44
8.	APPENDIX	53
8.1.	List of figures	53
8.2.	List of tables	53

ABBREVIATION

AC	Amacrine cells
BC	Bipolar cells
Brn3a	Brain-specific homeobox/POU domain protein 3A
BSA	Bovine serum albumin
CNS	Central nervous system
dRGC	Displaces retinal ganglion cells
GCL	Ganglion cell layer
GS-IB4	Isolectin B4
H&E	Hematoxylin and eosin
H ₂ O ₂	Hydrogen peroxide
HC	Horizontal cells
hESC	Human embryonic stem cells
INL	Inner nuclear layer
IOP	Inner ocular pressure
IPL	Inner plexiform layer
ipRGCs	Intrinsically photosensitive RGCs
LGN	lateral geniculate nucleus
MG	Müller glia
NBL	Neuroblastic layer
O ₂ ⁻	Superoxide anion
OCT	Optimal cutting temperature
-OH	Hydroxyl radicals
ON	Optic nerve
ONC	Optic nerve crush
ONL	Outer nuclear layer
OPL	Outer plexiform layer
PAX6	Paired Box 6
PBS	Phosphate-buffered saline
PFA	Paraformaldehyde
PR	Photoreceptors
RBPMS	RNA-binding protein with multiple splicing
Rbpms2	RNA-binding protein 2
RBPs	RNA-binding proteins
RGCs	Retinal ganglion cells

ROS	Reactive oxygen species
RPC	Retinal progenitor cells
RRM	RNA recognition motif
SEM	Standard error of the mean
SMI-32	Neurofilament H
TUJ1	Class III beta-tubulin
WT	Wild-type

1. Deutsche Zusammenfassung

Das RNA-bindende Protein mit multiplen Spleißvarianten (RBPMS), ein bekannter Marker für retinale Ganglienzellen (RGCs), ist in Bezug auf seine Rolle während der embryonalen Netzhautentwicklung, des Alterungsprozesses und bei neurodegenerativen Erkrankungen noch nicht vollständig verstanden. Ziel dieser Studie ist es, die Auswirkungen von Rbpms auf die Entwicklung der Netzhaut sowie auf pathologische Veränderungen im Zusammenhang mit neurodegenerativen Zuständen und Alterung zu untersuchen.

Durch Immunfärbungen von RBPMS und Brn3a an Netzhautabschnitten alternder Mausmodelle, die oxidativem Stress und erhöhtem hydrostatischem Druck ausgesetzt waren, sowie durch die Analyse von Augengewebe von Wildtyp (WT) und Rbpms-Knockout-Embryonen konnte festgestellt werden, dass RBPMS vorwiegend im Zytoplasma der RGCs in der Ganglienzellschicht lokalisiert ist. Die Ergebnisse zeigen, dass die Dichte und Immunreaktivität von RBPMS-positiven RGCs bei Mäusen mit zunehmendem Alter und unter Stressbedingungen abnimmt. Das Fehlen von Rbpms führte zu einer Reduktion der PAX6+-Zellen und Iba1+-Mikroglia, was auf eine zentrale Rolle von Rbpms bei der Spezifikation von RGCs aus retinalen Vorläuferzellen (RPCs) sowie bei der Koordination von neuronalen Überlebens- und Regenerationsprozessen hinweist. Dies resultierte in einer dosisabhängigen Abnahme der Dichte von Brn3a-positiven RGCs und des SMI-32-Arealanteils.

Es wurden jedoch keine signifikanten Unterschiede in der Zellanzahl der NBL-Schicht oder im Anteil der TUJ1+-Primärneuronen zwischen *Rbpms*^{-/-} und WT-Netzhäuten festgestellt, was darauf hindeutet, dass ein Mangel an Rbpms die Schichtbildung der Netzhaut verzögert, ohne die gesamte Morphologie des Auges zu beeinflussen. Diese Studie unterstreicht die essenzielle Funktion von RBPMS, dessen Expression mit Alterung und neurodegenerativen Veränderungen abnimmt, und hebt seine bedeutende Rolle bei der Differenzierung von RPCs zu spezifischen neuronalen Zelltypen hervor.

2. Summary

The RNA-binding protein RBPMS, characterized by multiple splicing variants and widely recognized as a marker for retinal ganglion cells (RGCs), has a role in embryonic retinal development, aging processes, and neurodegenerative conditions that remain incompletely understood. This research seeks to clarify the role of *Rbpms* in retinal development and to investigate its pathological changes in the context of aging and neurodegenerative diseases. By employing immunolabeling of RBPMS and Brn3a on retinal sections from aging mouse models under oxidative stress and elevated hydrostatic pressure and analyzing ocular tissue from wild-type (WT) and *Rbpms* knockout embryos, we observed that RBPMS predominantly resides in the cytoplasm of RGCs in the ganglion cells layer. Our findings show decreased RBPMS-positive RGC density and immunoreactivity with age and under stress conditions in mice. The absence of *Rbpms* disrupted the number of PAX6+ cells and Iba1+ microglia, suggesting a crucial role in RGC specification from retinal progenitor cells (RPC) and coordinating neuronal survival and regeneration. This resulted in a significant reduction in the density of Brn3a-positive RGCs and the SMI-32 area fraction. However, no significant difference in the NBL layer cell numbers or TUJ1+ primary neurons between *Rbpms*^{-/-} and WT retinas was observed, indicating that *Rbpms* deficiency delays retinal layering without altering overall ocular morphology. This study highlights the essential function of RBPMS in the expression decline during aging and neurodegeneration, underscoring its significant role in guiding RPC differentiation towards specific neural lineages.

3. INTRODUCTION

3.1. RBPMS expression in the retina of mammals and non-mammals

RNA-binding proteins (RBPs), crucial for post-transcriptional gene expression control, are essential in processing mRNA, regulating its transport, ensuring cellular localization, and facilitating translation ¹. RNA-binding protein with multiple splicing (RBPMS) is distinguished by possessing a singular RNA recognition motif (RRM) and is conserved across various species, also referred to as HERMES ^{2,3}. Studies have reported Hermes/RBPMS immunoreactivity localized in the axons and bodies of retinal ganglion cells (RGCs) in embryonic *Xenopus laevis* and zebrafish ^{2,4}, suggests a conserved pattern of expression across both non-mammalian and mammalian retinas. Moreover, Natic Piri et al., using semi-quantitative qRT-PCR, identified elevated expression of the Hermes gene in the retina, heart, kidney, and liver, while no significant expression was detected in other tissues ³.

In the African clawed toad, RGCs located in the innermost layer begin their differentiation in the dorsal region at approximately stage 34 ². This differentiation then progresses ventrally across the entire cell layer and, by stage 38, results in the expression of *Hermes* throughout the retina ². The expression of the *Hermes* gene in the eye is restricted to RGCs and is not detectable in bipolar cells and photoreceptors ².

Moreover, a comparative analysis of gene expression patterns in axotomized and control rat retinas demonstrated down-regulation of *Hermes* with multiple splicing in RGC-deficient retinas, as well as *Hermes* gene expression restricted to the ganglion cell layer (GCL) ³. RBPMS strongly and exclusively labels RGCs and displaces RGC (dRGC) somatic cells in the retinas of mice, rats, guinea pigs, rabbits, and monkeys ⁵. Thus, RBPMS is selectively expressed in RGCs and has been proposed as a marker for quantifying RGCs in normal retinas and estimating RGC loss in ocular neuropathy ⁶.

3.2. RBPMS has the potential to regulate the development of RGCs in the retina of vertebrates.

The retina is a sensory organ harboring six major neuronal cell types (optic rod, optic cone, horizontal, bipolar, anaphase, and RGCs) in response to intrinsic and extrinsic cues from the multipotent retinal progenitor cell (RPC) population in a stereotypical but overlapping temporal birth order ^{7,8}. RGCs serve as the retina's sole output neurons, responsible for receiving visual signals from photoreceptors through intermediary neurons and transmitting these integrated signals to other regions of the brain via their axons ⁹.

In developing mice, the majority of RGCs, exceeding 95%, originate within embryonic (E) days 12 to 17¹⁰⁻¹³. During this period, intrinsic transcriptional mechanisms and structural reorganization are crucial in guiding their development and connectivity⁹. In vertebrates, RGCs consistently represent the earliest cohort of neurons to emerge or initiate differentiation within the retinal architecture. In rhesus monkeys, RGC originates from E30⁷. In zebrafish embryos, the first BrdU-positive postmitotic cell was detected in the ventral nasal retinal GCL, near the optic rod, at 28 h after fertilization¹⁴. In the African clawed toad, a similar deuterated thymidine injection study localized the birth date of the RGC between stages 24 and 29¹⁵. The initial RGC was observed near the ON papilla at E2 in chicks¹⁶. Observations in mice revealed the emergence of RGCs occurring between embryonic E11 and E12, as determined by labeling with BrdU injection and rhodamine-dextran tracing¹⁰. Transcriptomic analyses of early embryonic retinas in humans and mice reveal similar developmental abnormalities, with neurogenesis of human RGCs starting at D52¹⁷. Initially, all newly formed RGCs aggregate in a concentrated region around the prospective ON papilla, situated at the center of the developing retina^{10,16}. Consequently, the differentiation of RGCs commences within the central area of the retina and advances outward toward the peripheral regions.

During embryonic development, *Rbpms* controls the translation of vital elements of cardiac commitment in human embryonic stem cells (hESC), providing a rich signaling infrastructure for cardiac mesoderm development through selective mRNA translation¹⁸. The processes of neuronal maturation and synaptic activity depend on effective post-transcriptional mechanisms to guide specific neuronal cell type differentiation and to promptly adjust to shifting neuronal needs¹⁹. Moreover, control at the transcriptional level is crucial for constructing and preserving the structural and functional intricacies of the central nervous system (CNS)¹⁹. The delivery of mRNAs to distal neuronal processes, such as dendrites and axons, plays essential roles in neural development, synaptic function, and plasticity²⁰. *Rbpms* is thought to contribute to regulating the stability and translation of transporter RNAs that are responsible for axon formation²¹ and axon arborization in *Xenopus* and zebrafish embryos⁴. *Rbpms* was associated with RGC differentiation in single-cell RNA sequencing datasets of the developing retina²²⁻²⁵. At embryonic day 14.5, RBPMS and RBPMS2 mRNA localizes to the GCL in the mouse retina²⁶. The occurrence of *Hermes* transcripts in the eye corresponds with successive waves of RGC differentiation as they progress through the retinal cell layer². However, the role of *Rbpms* in the developmental regulation of RGCs in the embryonic retina remains to be elucidated.

3.3. RBPMS could act as a marker for RGC degeneration

Neuronal loss was traditionally viewed as a standard feature of "normal" aging²⁷⁻²⁹. As part of the CNS, the retina, in addition to its accessibility, is regarded as a precious tissue for studying neurodegenerative diseases. The retina is now regarded as a gateway to the brain, providing a non-invasive approach for the early detection of neurodegenerative damage in various CNS disorders, including those not directly associated with visual system impairments, such as Alzheimer's and Parkinson's diseases^{30,31}. RGCs are a crucial type of neuron within the retina, with their axons connecting our eyes to the brain. These RGCs are targeted in common CNS diseases³², including the highly prevalent glaucoma³³, where their loss often leads to visual impairment or even blindness.

Identifying RGCs and entire RGC populations enables a range of experimental studies^{34,35}. As an illustration, investigations into CNS injury often employ the visual system as a paradigm, with experimental interventions typically involving quantifying and distributing RGCs. Immunohistochemical techniques for identifying RGCs present a favorable option over retrograde tracing, providing various benefits, such as reducing tissue injury caused by experimental procedures and enabling more precise labeling of the complete RGC population. Therefore, there is excellent value in possessing a proprietary marker for RGCs to identify the entire RGC population.

In the retina, RBPMS and Brn3a (a reliable, efficient *ex vivo* marker of RGCs³⁶) expression levels reflect the physiological state of RGCs, and they decrease as RGCs enter apoptosis³⁷, acting as viability markers for RGCs. Furthermore, not all Brn3a-positive cells are RBPMS+. The critical distinction between RBPMS and Brn3a lies in their expression patterns: Brn3a is found in vision-forming RGCs, which constitute 91% to 98% of RGCs depending on the species, but it is not present in intrinsically photosensitive RGCs (ipRGCs), which make up 2% to 7.5% of the RGC population^{38,39}, and that ipRGCs are RBPMS+ Brn3a-⁴⁰. A recent study has shown that RBPMS migrates from RGC somatic cells to dendrites in response to aging or hypoxia⁴¹. It is well-established that post-transcriptional regulation is crucial for neuronal maturation, maintenance, and function⁴². Although RBPMS might be associated with neuronal survival and plasticity, a comprehensive and systematic understanding remains elusive, particularly regarding age-associated neuronal decline and pathological alterations in retinal neurodegenerative diseases.

3.4. Glaucoma

Glaucoma is recognized as a neurodegenerative condition affecting both the eye and brain ⁴³. It leads to RGC dysfunction and progressive loss, which underpins blindness in 80 million individuals ^{44,45}. This complex, multifactorial disease is largely driven by increased intraocular pressure (IOP) and the aging process, both recognized as major risk factors ^{46,47}. Additionally, factors such as physical injury to ON fibers, oxidative stress, and low oxygen levels have been identified as contributors to glaucoma's pathogenesis through their roles in promoting RGC mitochondrial dysfunction, glial activation, and neuroinflammation ⁴⁸.

BPMS is abundantly expressed in RGCs ^{2,3}, and its antibodies help assess RGC numbers in chronic disease models (such as glaucoma) or following acute injuries (like ON damage or retinal ischemia) ³⁴. These antibodies also facilitate identifying therapeutic agents to mitigate or prevent RGC degeneration. BPMS antibodies are useful for identifying and characterizing RGCs in cell culture settings. Furthermore, the *Bpms* gene also plays a valuable role in directing RGC-specific expression within transgenic animal systems and serves as a marker in gene therapy mediated by viral vectors.

Therefore, this study seeks to investigate how *Bpms* deficiency influences the specification of RGCs during eye development, as well as the pathological alterations in RGCs in aging and neurodegenerative diseases. To this end, we utilize the retinas of *Bpms* knockout embryos and aging mice, including pathological injury paradigms.

4. Materials and Methods

4.1. Animals Used in Experiments

All experimental protocols complied with the guidelines specified in the Declaration of Helsinki and complied with the German Animal Welfare Act. The protocols involving animals in this study received evaluation and authorization from the agency overseeing animal welfare in North Rhine-Westphalia (LANUV, State Office for Nature, Environment, and Consumer Protection, approval number 81-02.04.2020. A490).

4.2. Aging mice

We utilized male C57BL/6J mice aged 8 weeks (young adult group, about 20 years of age on average for humans)⁴⁹, 30 weeks (middle age group), and 60 weeks (aged group⁵⁰). All animals were maintained in a pathogen-free environment using individually ventilated cage (IVC) systems (GM 500, Tecniplast® Greenline), with no more than five mice housed per cage. Adjust the lighting to a 12-hour light/dark schedule, beginning at 6 a.m., and ensure environmental conditions are maintained at 22 ± 2 °C with 45-65% relative humidity. The mice received a sterilized rodent diet free of phytoestrogens (Altromin 1314, containing 59% carbohydrates, 27% protein, and 14% fat) along with unlimited access to feed and acidified drinking water. In particular, an illumination level of 39 ± 7 lux was used to optimize the negative effects of standard feeder lighting on the retinas of the elderly^{51,52}.

4.3. Preparation of retinal explants

After euthanasia by cervical dislocation, the eyes of C57BL/6J mice were promptly extracted and placed into Petri dishes filled with cold, sterile phosphate-buffered saline (PBS) chilled on ice. The front segment of the eye was dissected to reveal the retina, allowing it to be carefully detached from the sclera. The entire retina was delicately removed away from the optic cup, with the vitreous body subsequently extracted. Subsequently, the retina explants were sectioned into four equal parts with the GCL oriented upwards and positioned on Millipore filters (Millipore; Millipore, Cork, Ireland). The retinal sections were then transferred into 35 mm Lumox Petri dishes (Sarstedt, Nümbrecht, Germany) and incubated in DMEM/F12 medium (Gibco BRL, Eggenstein, Germany) enriched with 10 µg/mL porcine insulin, 100 U/mL penicillin, and 100 µg/mL streptomycin. The cultures were maintained in an incubator set at 37°C within a moist atmosphere containing 5% CO₂ mixed with air. The retinal tissues were randomly allocated to a control group and two glaucoma model groups to reduce variability.

4.4. Elevated Hydrostatic Pressure Model

Retinal explants were placed in a custom-made pressure culture chamber to simulate intraocular conditions with an abnormally elevated IOP of 60 mmHg for 24 hours (n=6/age/group). The chamber, constructed from steel, features a screwable lid and a non-directional valve that permits the introduction of 5% CO₂ from the incubator to maintain or adjust the pressure as needed. Additionally, the air pressure within the hyperbaric incubator is continuously monitored by a manometer.

4.5. Oxidative Stress Model

A 300 µM concentration of hydrogen peroxide (H₂O₂) was introduced into the common culture medium of the retinal explants described above, followed by a 24-hour incubation in the incubator (n=6/age/group).

4.6. Generation and genotyping of *Rbpms* mutant mice

Rbpms mutant mice (*Rbpms*^{em1/Baz}) were produced through CRISPR/Cas9 genome editing at the CECAD *in vivo* Research Facility (ivRF, Branko Zevnik) following standard procedures of delivering a mixture of ribonucleoprotein complexes of guide RNA (gRNA), tracer RNA and Cas9 protein (iDT technologies) to fertilized zygotes by electroporation^{53,54}. The gRNA (TGGCCAAGAACAACACTCGTA) was designed *in silico* (Broad Institute website) in Exon 5 of *Rbpms*. The animals were reared and maintained under SOPF standards within the CECAD animal facility. Approval for animal generation (application number: 84 02.04.2014.A372) and breeding (application numbers: 84-02.04.2015.A405 and 81-02.04.2021.A130) was granted by LANUV NRW, Germany. The phenotypes of *Rbpms* mutant were examined on an FVB/NRj background. The genotyping procedure was conducted as follows: For the 1 bp insertion (C at the cut site), PCR with *Rbpms_gRNA_Ex5_F* and *Rbpms_gRNA_Ex5_R* primers, followed by restriction digest with TspgW1 (cuts mutant allele) at 70C for 4 h and run on a 1% gel. For the 17 bp deletion (TCGTAGGGACTCCAAAC), PCR with *Rbpms_gRNA_Ex5_F2* and *Rbpms_gRNA_Ex5_R2* primers and run on a 4% gel.

Table 1 of primers used:

<i>Rbpms_gRNA_Ex5_F</i>	CATTCTGGTTTACATCTTCCCCT	265 bp
<i>Rbpms_gRNA_Ex5_R</i>	CACCTCTTAACAGTCCTTTGCT	
<i>Rbpms_gRNA_Ex5_F2</i>	TTTTCTTCCAAAGGGCATCC	160 bp
<i>Rbpms_gRNA_Ex5_R2</i>	CTCCCTGGCAATGAACTGAG	

4.7. Immunohistochemistry

4.7.1. Tissue preparation

The retinal explants were rinsed with PBS and immersed in 4% paraformaldehyde (PFA) solution (Histofix, Roth, Karlsruhe, Germany) for 30 minutes to ensure proper fixation and then placed in a PBS-based 30% sucrose solution to incubate overnight. They were then placed on black filter paper for preparation as retinal flat mounts. Similarly, the embryo heads were rinsed in PBS, immersed in 4% PFA for fixation overnight, and then transferred to a 30% sucrose solution to incubate overnight. Once fixed, the retinas and heads were preserved in optimal cutting temperature (OCT) compound (Sakura Finetek, Torrance, CA, USA) to enable cryostat sectioning. Vertical sections of 12 μm thickness were prepared using a Leica CM3050S cryostat (Leica Microsystems, Buffalo Grove, IL). The prepared sections were placed onto gelatin-coated slides and stored frozen until further use in immunohistochemical analysis.

4.7.2. Histopathological analysis of embryonic retinas

Embryonic retinal cryosections, measuring 12 μm thick, were subjected to hematoxylin and eosin (H&E) staining for histological examination. The sections were then scanned on a Zeiss Imager M.2 microscope equipped with an Apotome.2, using 10x and 20x objectives for imaging.

4.7.3. Retinal flat mount RGC quantification

RGCs were quantified using double immunohistochemical staining with a rabbit anti-RBPMS antibody (Novus, NBP2-20112, Lot#130-96) and a mouse anti-Brn3a antibody (Millipore, MAB1585, Lot#3684607). Initially, the retinas were rinsed in PBS and then blocked in a solution of 0.3% Triton X-100 and 5% bovine serum albumin (BSA) in PBS for 30 minutes at ambient temperature. The samples were subsequently exposed to primary antibodies targeting RBPMS (1:300) and Brn3a (1:200) for 24 hours at 4°C. After incubation, the retinas were rinsed and subsequently treated with secondary antibodies, specifically goat anti-rabbit Alexa Fluor 546 IgG (1:1000) and goat anti-mouse Alexa Fluor 488 IgG (1:1000), for 1 hour at ambient temperature. The retinas were gently cleaned and placed on glass slides with the RGC layer oriented upward and secured using a DAPI-containing mounting medium (Vector Laboratories, Burlingame, CA). Retinal flat mounts were documented using a Zeiss Imager M.2 microscope equipped with an Apotome.2 (Carl Zeiss, Jena, Germany), and RGC morphology was examined at 20x magnification.

Lastly, three images were taken from each quadrant of the retina. A predefined template was centered on the optic disc of each retina, and the periphery was outlined to facilitate RGC

quantification in both the central and peripheral areas. The RGCs in each image were then counted using ImageJ software.

4.7.4. Immunofluorescence labeling in Embryo or Adult Retinal cryosections

Immunohistochemical staining was conducted using the indirect immunofluorescence technique. Retinal cryosections were treated with a blocking buffer composed of PBS, 10% goat serum, and 0.1% Triton X-100, applied at room temperature for 60 minutes. The primary antibodies (refer to Table 2) were prepared in the blocking buffer and left on the sections overnight at 4°C. Following incubation, the retinal cryosections were rinsed three times for 5 minutes each with PBS to eliminate any unbound antibodies. The relevant secondary antibody (see Table 2) was prepared in the blocking buffer and applied to the sections for 1 hour at room temperature in darkness, followed by three washes lasting 5 minutes each. All slides were then mounted with DAPI-containing VectaShield medium (Vector Laboratories, Burlingame, CA) to prepare for imaging. Fluorescence imaging of the retinal cryosections was performed using a TCS SP8 X Confocal Microscope (Leica, Wetzlar, Germany) and an Apotome.2-equipped Zeiss Imager M.2, both under a 20x objective. The images were analyzed using ImageJ2 version 2.3.0.

Table 2 Antibodies used for histological analyses

Antibodies	Manufacturer, Cat. No.	Dilution	Secondary antibodies
RBPMS (rabbit)	Novus, NBP2-20112, #130-96	1:300	GαRb A488 & 594, 1:1000, Invitrogen
Brn3a (mouse)	Millipore, MAB1585, #3684607	1:200	Gαm A488 & 594, 1:1000, Invitrogen
PAX6 (rabbit)	Abcam, ab5790	1:500	GαRb A594, 1:1000, Invitrogen
Iba1(rabbit)	Fujifilm, #019-19741	1:500	DαRb A647, 1:1000, Invitrogen
Anti-Neurofilament	Millipore, #N4142	1:200	GαRb A594, 1:1000, Invitrogen
Anti-beta III Tubulin antibody (2G10)	Abcam, ab78078	1:200	Gαm A488, 1:1000, Invitrogen

Isolectin GS-IB4	Invitrogen	1:500	Alexa Fluor 488 conjugate, Invitrogen
------------------	------------	-------	--

4.8. Analysis of Statistical Data

The data are presented as the mean \pm standard error of the mean (SEM), with 'n' indicating the number of animals included in each group. Statistical analyses and graph generation were carried out using GraphPad Prism software, version 9.0 (GraphPad, San Diego, CA). Statistical significance was determined by a p-value less than 0.05.

5. Results

5.1. Variation of RBPMS in response to aging

To elucidate the expression pattern of RBPMS in adult mice and during age-related neuronal functional decline, we visualized and quantified the localization of RBPMS and Brn3a within RGCs in adult and aging mice. Under normal physiological conditions in adult mice, RBPMS was localized in the cell bodies, whereas Brn3a localized in the nuclei of RGCs (Figure 1A), as expected for a transcription factor.

To investigate the impact of aging on RBPMS expression, we performed a quantitative analysis of RBPMS+ Brn3a+, RBPMS+ Brn3a-, and Brn3a+ RBPMS- RGCs density in retinal flat mounts at different ages (Figure 1B). Under normal physiological conditions, we observed a significant decline in the density of RBPMS+Brn3a+ RGCs at 60 weeks of age ($1137 \pm 178/\text{mm}^2$), which was almost half (46%) that at 8 weeks of age ($2122 \pm 134/\text{mm}^2$, $P=0.0003$) and about one-third (34%) that at 30 weeks of age ($1732 \pm 55/\text{mm}^2$, $P=0.0163$) (Figure 1C).

Moreover, at 8 weeks of age, the density of Brn3a+RBPMS- RGCs ($275 \pm 25/\text{mm}^2$) was significantly lower compared to the density of RBPMS+ Brn3a- RGCs ($402 \pm 44/\text{mm}^2$, $P=0.0423$). Interestingly, the rate of decline of RBPMS+Brn3a- RGCs density with aging was higher than that of Brn3a+Rbpms- RGCs, which remained relatively stable. When comparing the densities at 60 weeks to those at 8 weeks, we found that Brn3a+RBPMS- RGCs exhibited a 55% loss ($123 \pm 19/\text{mm}^2$), while the density loss of RBPMS+Brn3a- RGCs was as high as 48% ($209 \pm 28/\text{mm}^2$) (Figure 1C).

To further investigate the spatial distribution of the diminished RBPMS expression across the retina with aging, we quantified the density of various subpopulations of RGCs in the central, middle, and peripheral regions (Figure 1D). We observed that the loss of RBPMS was more prominent in the retina's peripheral regions than in the central areas. Specifically, comparing the densities of RBPMS+ Brn3a-RGCs at 60 weeks to those at 8 weeks, the data showed a loss of 50% in the central region, 26% in the middle region, and 67% in the peripheral region. On the other hand, compared to the 30-week age group, the 60-week group lost 55% of RBPMS+ Brn3a- RGCs in the peripheral region (Figure 1E, Table 3).

The findings indicate a regional vulnerability of RBPMS-expressing RGCs to age-related degeneration, with a more significant decline in the peripheral areas of the retina.

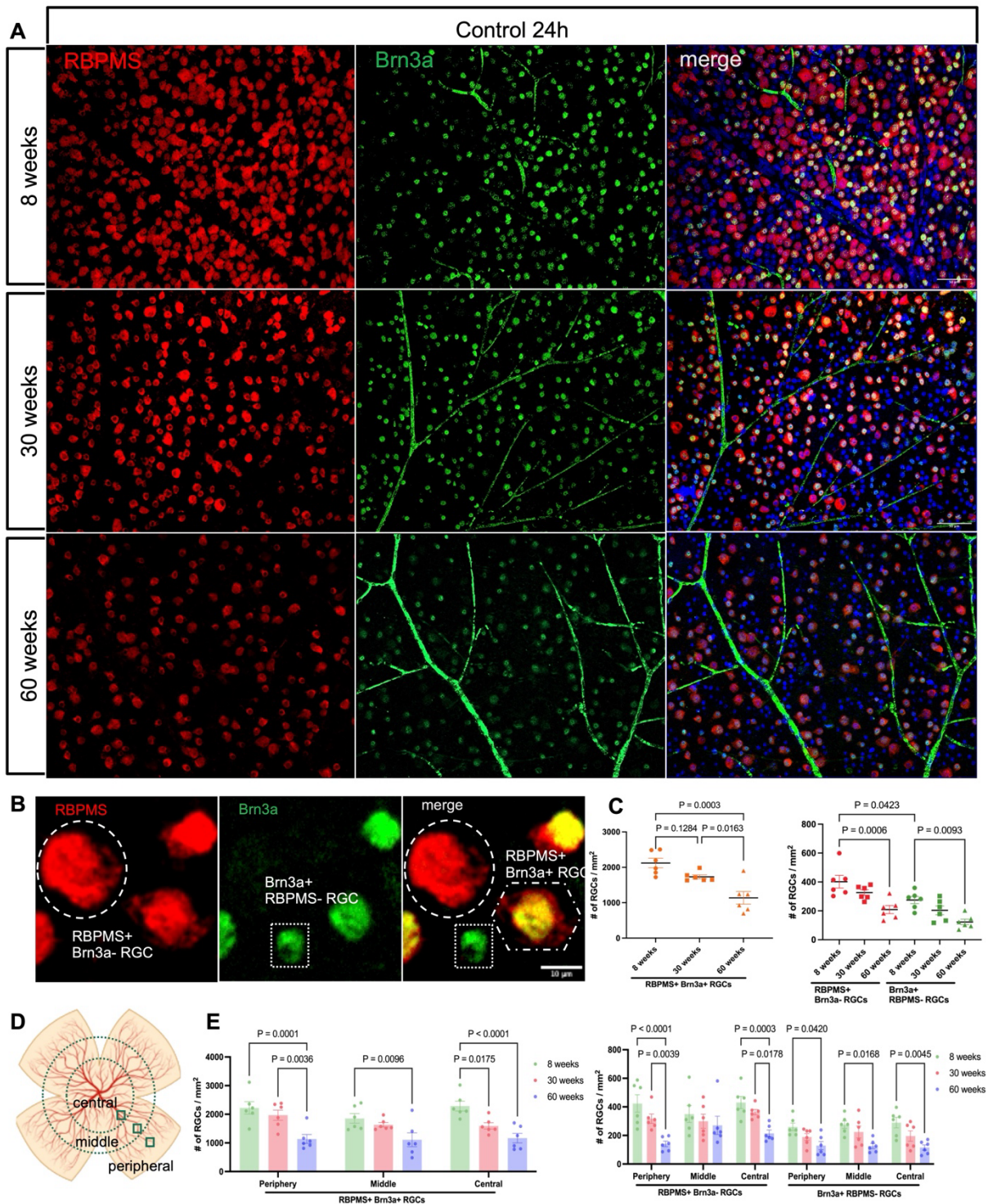


Figure 1 Variation of RBPMS in response to aging in the retinal flat mounts of *C57BL/6J* mice. Representative images of immune labeled by RBPMS (red) and Brn3a (green) in the retinal flat mounts of aging *C57BL/6J* mice under control 24h. Scale bars equal 50 μ m. (B) The schematic diagram of RBPMS+Brn3a+RGCs, RBPMS+Brn3a-RGCs, and Brn3a+RBPMS-RGCs. Scale bars equal 10 μ m. (C) Statistical analysis demonstrated that 60 weeks retinas demonstrated a notable decline in the density of RBPMS+Brn3a+RGCs, RBPMS+Brn3a-RGCs, and Brn3a+RBPMS-RGCs compared to the 8 weeks retinas. (D) The schematic diagram of the retina's central, middle, and peripheral regions. (E) Statistical analysis

demonstrated that 60 weeks of retinas showed a marked reduction in the density of RGCs compared to the 8 weeks of retinas, especially in the peripheral areas of the retina. $n = 6$ in each group. Error bars represent the mean \pm SEM, and differences were evaluated through one-way ANOVA followed by Tukey's test for multiple comparisons.

5.2. RBPMS loss in retinal neurodegenerative diseases

5.2.1. RBPMS expression decreases under elevated hydrostatic pressure

To characterize the response of RBPMS+ RGCs to high hydrostatic pressure during aging, we examined the RBPMS+ RGCs under elevated hydrostatic pressure (60mmHg) conditions at different ages (Figure 2A).

RBPMS+Brn3a+RGCs decreased by 38% ($1326 \pm 103/\text{mm}^2$) in the 8-week group, 33% ($1155 \pm 81/\text{mm}^2$) in the 30-week group, and 40% ($687 \pm 54/\text{mm}^2$) in the 60-week group after high hydrostatic pressure compared with the age-appropriate control group. The loss of RBPMS+ Brn3a+ RGCs under hyperbaric pressure was predominantly distributed in the peripheral region of the retina, especially at 60 weeks. Interestingly, only RBPMS+ Brn3a-RGCs were significantly reduced after hyperbaric pressure in all age groups (8 weeks: $128 \pm 29/\text{mm}^2$, 30 weeks: $120 \pm 12/\text{mm}^2$, 60 weeks: $73 \pm 5/\text{mm}^2$), with the loss characteristically distributed uniformly in the three regions of the retina. The density of Brn3a+ RBPMS- RGCs was significantly lower after hyperbaric pressure only in the intermediate region at 30 weeks. However, it did not change significantly in the other age groups compared to the control group (Figure 2B, Table 3).

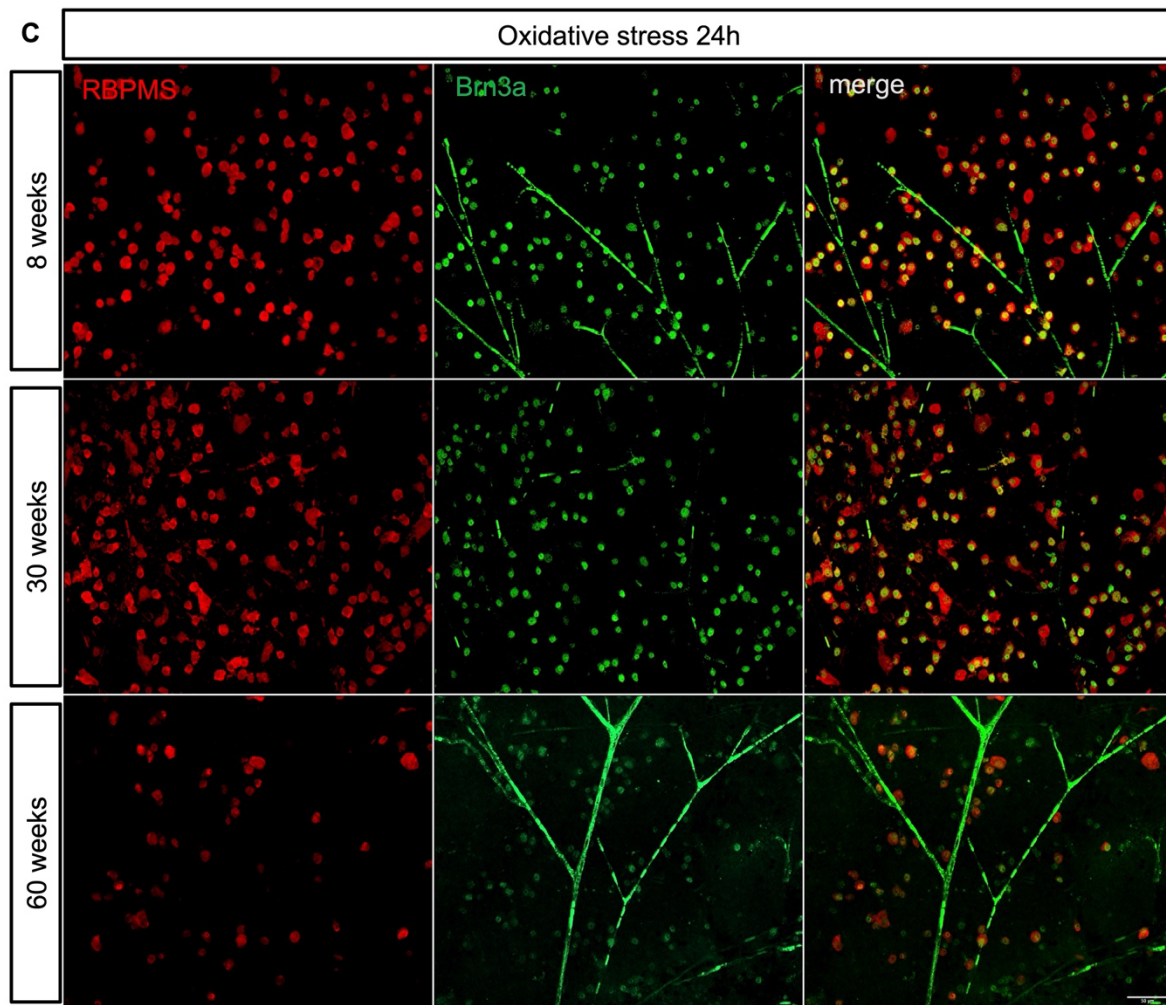


Figure 2 RBPMS expression decreases under elevated hydrostatic pressure and oxidative stress.

(A) Representative images of immune labeled by RBPMS (in red) and Brn3a (in green) in the retinal whole mounts of aging *C57BL/6J* mice under elevated hydrostatic pressure 60mmHg 24h. Scale bars equal 50 μ m. (B) Statistical analysis demonstrated that the retinas under high hydrostatic pressure and oxidative stress showed a notable decline in the density of RBPMS+Brn3a+RGCs and RBPMS+Brn3a-RGCs compared to the Control retinas, especially in the peripheral areas of the retina. (C) Representative images of immune labeled by RBPMS (in red) and Brn3a (in green) in the retinal flat mounts of aging *C57BL/6J* mice under 300 μ M H_2O_2 24h. Scale bars equal 50 μ m. $n = 6$ in each group. Error bars represent the mean \pm SEM, and differences were evaluated through one-way ANOVA followed by Tukey's test for multiple comparisons.

5.2.2. RBPMS expression declines under oxidative stress

An overproduction of reactive oxygen species (ROS), including superoxide anions (O_2^-), hydrogen peroxide (H_2O_2), and hydroxyl radicals ($-OH$), is a defining feature of oxidative stress.

We used 300 μM H_2O_2 to directly drive oxidative stress in the retina. Exposed to oxidative stress, the survival rate of both RBPMS+ Brn3a+ RGCs was significantly lower than controls (Figure 2C). RBPMS+ Brn3a+ RGCs were lost uniformly in all regions of the retina at 8 weeks and 30 weeks, whereas the loss of RBPMS+ Brn3a+ at 60 weeks occurred only in the intermediate regions.

Compared with the control group, the exposure to H_2O_2 resulted in a decrease in the survival density of RBPMS+ Brn3a- RGCs at all stages of age (8 weeks: $162 \pm 32/\text{mm}^2$, 30 weeks: $105 \pm 13/\text{mm}^2$, 60 weeks: $105 \pm 12/\text{mm}^2$) (Table 3). The results revealed that RBPMS+ Brn3a- RGCs were lost under oxidative stress in all age groups, yet their loss distribution varied across ages. At 8 and 30 weeks, the loss of RBPMS+ Brn3a- RGCs was uniformly distributed across all regions of the retina. At 60 weeks, on the other hand, the loss was significantly concentrated in the middle and central regions. For Brn3a+ RBPMS- RGCs, the loss occurred only at 30 weeks and only in the central and intermediate regions (Figure 2B, Table 3).

The results indicate that RBPMS expression is significantly decreased when exposed to high hydrostatic pressure and oxidative stress, where the loss distribution is more pronounced in the peripheral region of the retina.

Table 3 The density of different types of RGCs in various regions of the retina throughout aging and neurodegeneration

RGCs Type /mm ²	Regio n of retina	8 weeks			30 weeks			60 weeks		
		Cont rol	Press ure	H ₂ O ₂	Cont rol	Press ure	H ₂ O ₂	Cont rol	Press ure	H ₂ O ₂
RBPMS + Brn3a+ RGCs	periph	2223	1121±	1235	1968	821±8	971±1	1136	493±4	642±
	entral	±217	249	±127	±177	0	41	±156	0	133
	middle	1856	1559±	1032	1634	1118±	971±9	1110	688±8	516±
RBPMS + Brn3a- RGCs	central	±167	214	±173	±78	88	6	±242	0	142
	entral	2286	1298±	1192	1595	1526±	1118±	1166	881±6	819±
	entral	±170	195	±110	±110	157	118	±166	0	168
RBPMS + Brn3a- RGCs	average	2122	1326±	1153	1732	1155±	1020±	1137	687±5	659±
	verage	±134	103	±106	±55	81	86	±178	4	82
	periph	424±	101±3	120±	317±	94±13	101±1	141±	62±14	95±1
RBPMS + Brn3a- RGCs	entral	61	4	32	33		2	19		6
	middle	350±	143±2	198±	299±	128±1	105±1	271±	87±16	127±
	entral	59	3	47	49	8	2	64		24

	central	430±	139±3	166±	363±	140±2	110±2	215±	70±6	95±1
		43	7	46	19	8	9	23		0
	average	402±	128±2	162±	327±	120±1	105±1	209±	73±5	105±
		44	9	32	19	2	3	28		12
Brn3a+	periph	260±	190±5	144±	189±	148±2	130±1	129±	78±14	119±
RBPMS	eral	27	0	26	24	4	4	29		22
-RGCs	middle	275±	146±2	154±	225±	103±9	80±20	125±	90±16	121±
		26	6	52	41			18		11
	central	290±	204±5	154±	196±	142±1	91±13	116±	89±16	129±
		36	1	38	36	2		19		22
	average	275±	180±2	151±	203±	131±9	100±1	123±	86±7	123±
		25	3	26	30		2	19		9

5.3. Characteristics and Spatial Distribution of Structural Features of Rbpms in Age-Related Retinal Neurodegeneration

A study demonstrated that RBPMS is mainly found in the cell bodies within the retina under normal conditions. However, during hypoxia, its localization changes, appearing in RGC dendrites situated in the inner plexiform layer (IPL) ⁴¹. Therefore, we sought to examine the characteristics and spatial distribution of structural features of RBPMS in age-related retinal neurodegeneration by observing the expression and localization of RBPMS in retinal cross-sections under different conditions.

The results revealed that RBPMS was distributed in the cytoplasm under normal physiological conditions, and its fluorescence intensity was significantly reduced at 60 weeks. RBPMS was localized in the GCL of the retina, which did not change with aging (Figure 3A, B). In retinas exposed to increased hydrostatic pressure and oxidative stress, it was observed that RBPMS remained confined to the cytoplasm of RGCs, with a notable reduction in fluorescent intensity following injury (Figure 3C). However, the spatial distribution of RBPMS in retinal cross-sections under both injury conditions was not altered compared with physiological conditions. These data demonstrate that RBPMS does not change its spatial distribution but responds to

aging and retinal neurodegeneration by a decrease in expression.

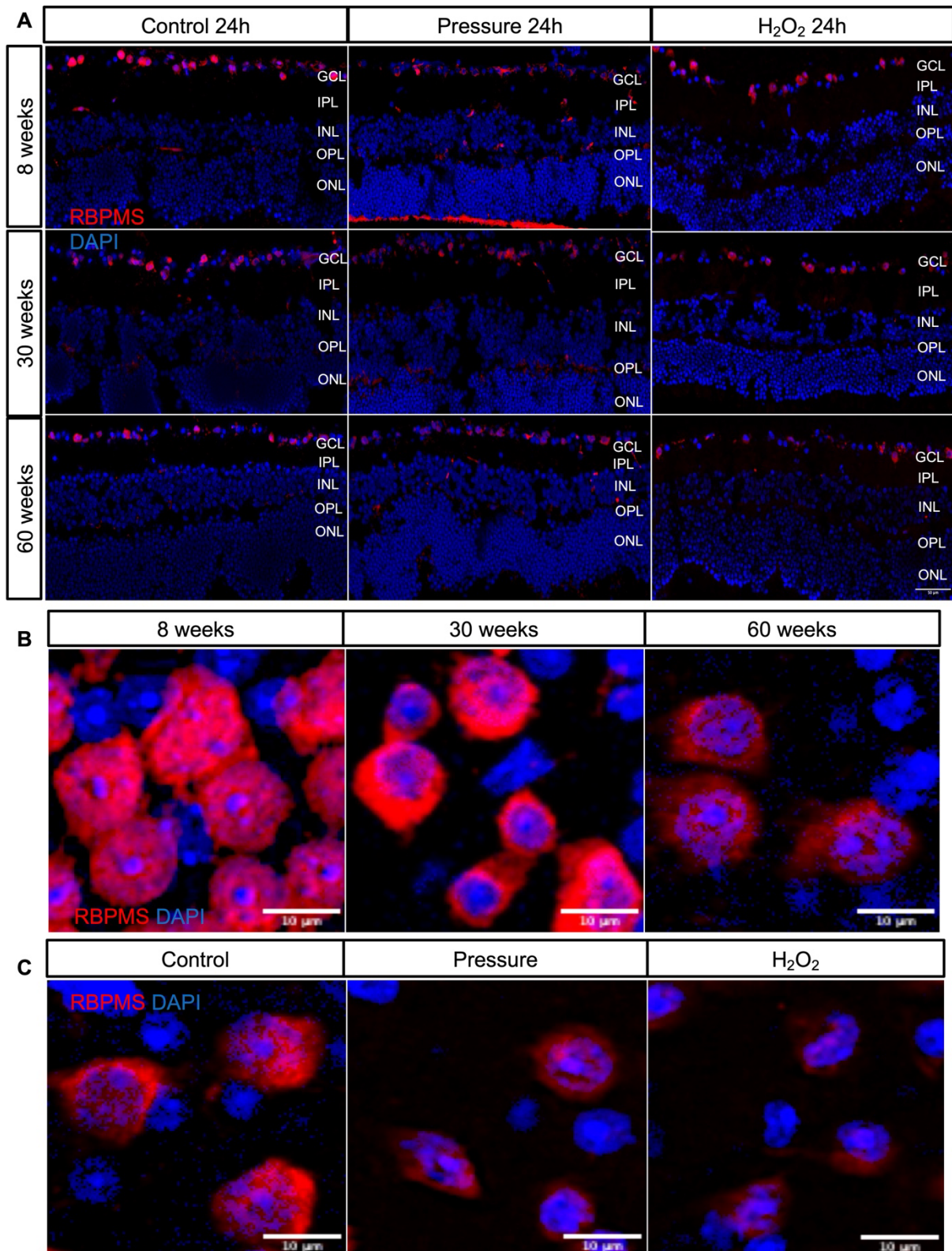


Figure 3 Characteristics and spatial distribution of structural features of *Rbpms* in age-related retinal neurodegeneration.

(A) Representative images of RBPMS-labeled RGCs (red) with DAPI nuclear staining (blue) in retinal cryosections of aging C57BL/6J mice under control, elevated hydrostatic pressure,

and oxidative stress. Scale bars represent a length of 50 μm . Representative images of RBPMS-labeled RGCs (red) with DAPI nuclear staining (blue) in retinal flat mounts of aging C57BL/6J mice under (B) control, (C) elevated hydrostatic pressure and oxidative stress. Scale bars equal 10 μm .

5.4. RBPMS expression in the GCL of the embryonic retina

Given the specificity of RBPMS expression in the cytoplasm of human RGCs, its expression levels decline with aging and pathological changes. Additionally, *Rbpms* is considered to contribute to the development of neuronal axons. We propose a hypothesis: Does *Rbpms* participate in the regulation of RGC development during the embryonic stage? To determine the expression and spatial distribution of RBPMS in the embryonic retina, we co-labeled the embryonic retina with RBPMS and Brn3a at E16.5. RBPMS and Brn3a immunoactivity co-localized in the retinal flat mounts and the GCL layer of the E16.5 retina in frozen sections (Figure 4A, B). These results confirm that RBPMS marks the GCL layer during mouse retinal development.

To explore the function of *Rbpms* in retinal development, we used CRISPR/Cas9 to generate *Rbpms*^{-/-} mice (see Methods). The genotype of the embryos with a 17 bp deletion in Exon 5 was confirmed by PCR to distinguish the WT and mutant alleles (Figure 4C). *Rbpms*^{-/-} embryos arrested development in the third trimester and before birth. A comparison of the eyes of *Rbpms*^{-/-} and their control littermates from E13.5 to E17.5 showed that optic cup formation was largely unaffected in *Rbpms*-deficient embryos (Figure 4D). Immunofluorescence staining showed no RBPMS-positive signal in the *Rbpms*^{-/-} retina (Figure 4D).

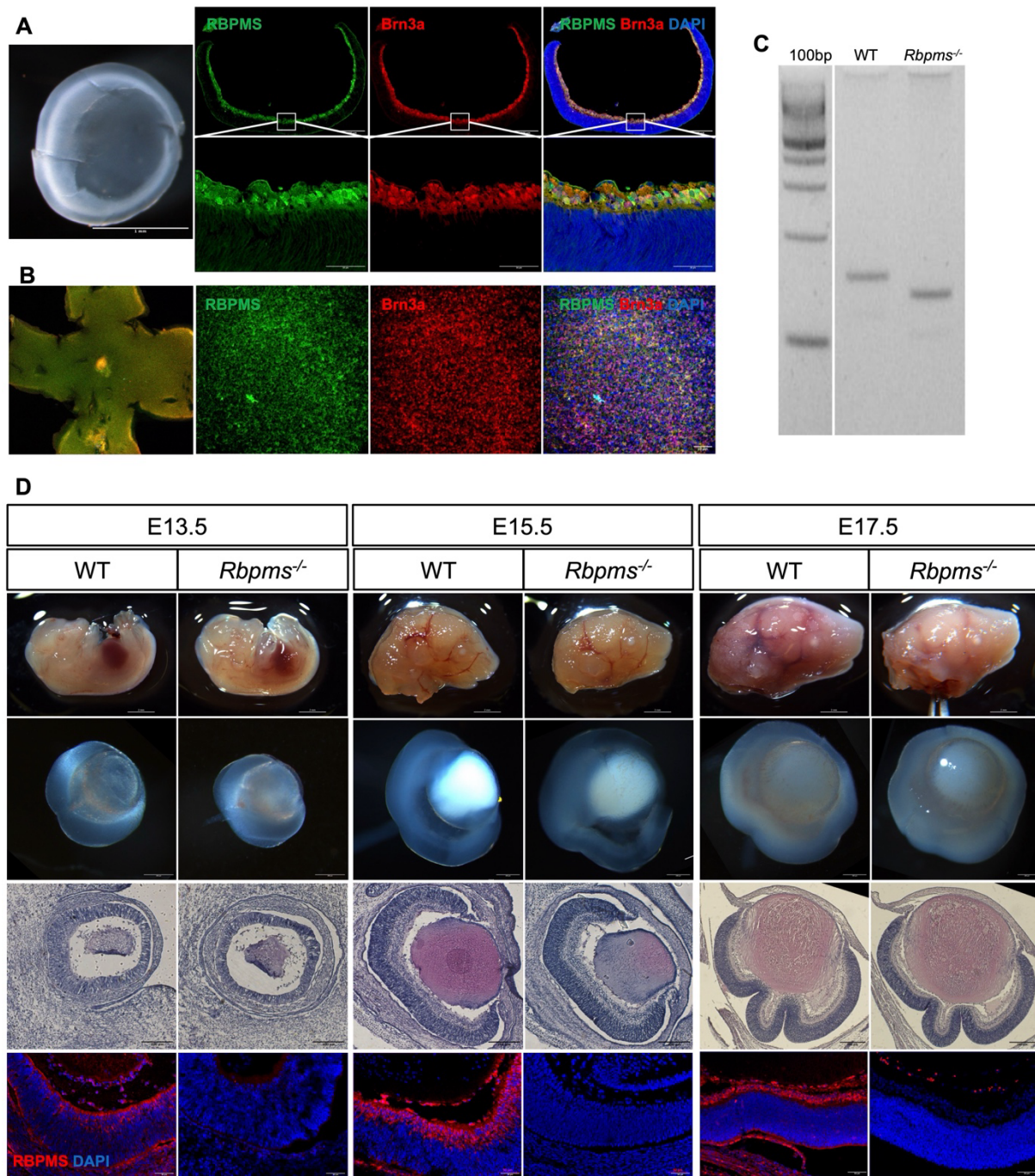


Figure 4 RBPMS expression within the GCL of the developing retina.

(A) Retinal cryosections of embryos (Scale bars equal 100 μ m), and (B) Embryonic retinal flat-mounts were immunolabeled using anti-RBPMS (green) and anti-Brn3a (red) antibodies, with DAPI (blue) for nuclear staining (Scale bars: 50 μ m). The lower panels in (A) show magnified images of the boxed areas (Scale bars: 50 μ m). (C) RT-PCR confirmed the genotype of the embryos to distinguish WT and *Rbpms* KO fetal mice. (D) The head and isolated eyeball from WT and *Rbpms*^{-/-} littermates fetal mice, and the H&E staining with eyeballs from E13.5 to E17.5. Scale bars equal 2 mm in the images of heads. Scale bars equal 200 μ m in the images of the eyeball and H&E staining. Cryosections of the retinas from WT and *Rbpms*^{-/-} embryos were

stained with anti-RBPMS (red) and counterstained with DAPI (blue) for nuclei. Scale bars represent 50 μm .

5.5. *Rbpms* deletion causes delayed development of embryonic retinal lamination patterns.

To assess the impact of *Rbpms* deficiency on retinal development, we first observed the lamination patterns of the retina at E15.5 and E17.5. In H&E staining of retinas, we observed that the lamination patterns of *Rbpms*-deficient retinas appeared to show no progression from E15.5 to E17.5. In contrast, the lamination patterns of the WT retinas exhibited significant development during this period (Figure 5A). Measurements of the thickness of each layer of the retina, as shown in Figure 5B, indicate that at both E15.5 and E17.5, the total thickness and GCL of the *Rbpms*^{-/-} retina (E15.5: $152 \pm 4.5\mu\text{m}$; E17.5: $144 \pm 1.9\mu\text{m}$) was slightly thinner than that of the WT (E15.5: $176 \pm 4.4\mu\text{m}$; E17.5: $189 \pm 1.3\mu\text{m}$), while the IPL showed no difference (Figure 5B).

E17.5 retina had differentiated into four layers in WT and *Rbpms*^{-/-} embryos (Figure 11A). The amacrine cells (AC) layer in the WT retina was differentiated and clearly delineated, while in contrast, the differentiating AC layer was faintly visible in the *Rbpms*-deficient retina ($14 \pm 1.4\mu\text{m}$) and significantly thinner than that in the WT retina ($28 \pm 1.3\mu\text{m}$) ($P=0.0003$) (Figure 5B). Furthermore, the neuroblastic cell layer (NBL) of the E17.5 *Rbpms*^{-/-} retina ($90 \pm 2.0\mu\text{m}$) was significantly thinner than that of the WT ($112 \pm 3.5\mu\text{m}$) (Figure 5B).

In addition, the density of cells in the GCL in *Rbpms*-deficient retinas (E15.5: $8284 \pm 177.1/\text{mm}^2$; E17.5: $6964 \pm 107.5/\text{mm}^2$) was significantly lower than in WT (E15.5: $11352 \pm 217.0/\text{mm}^2$; E17.5: $8459 \pm 49.33/\text{mm}^2$) ($P<0.0001$), whereas the density of RPC cells in the NBL layer was not significantly altered (Figure 5C). The findings indicate that the lamination pattern of *Rbpms*-deficient retinas exhibits developmental hindrance.

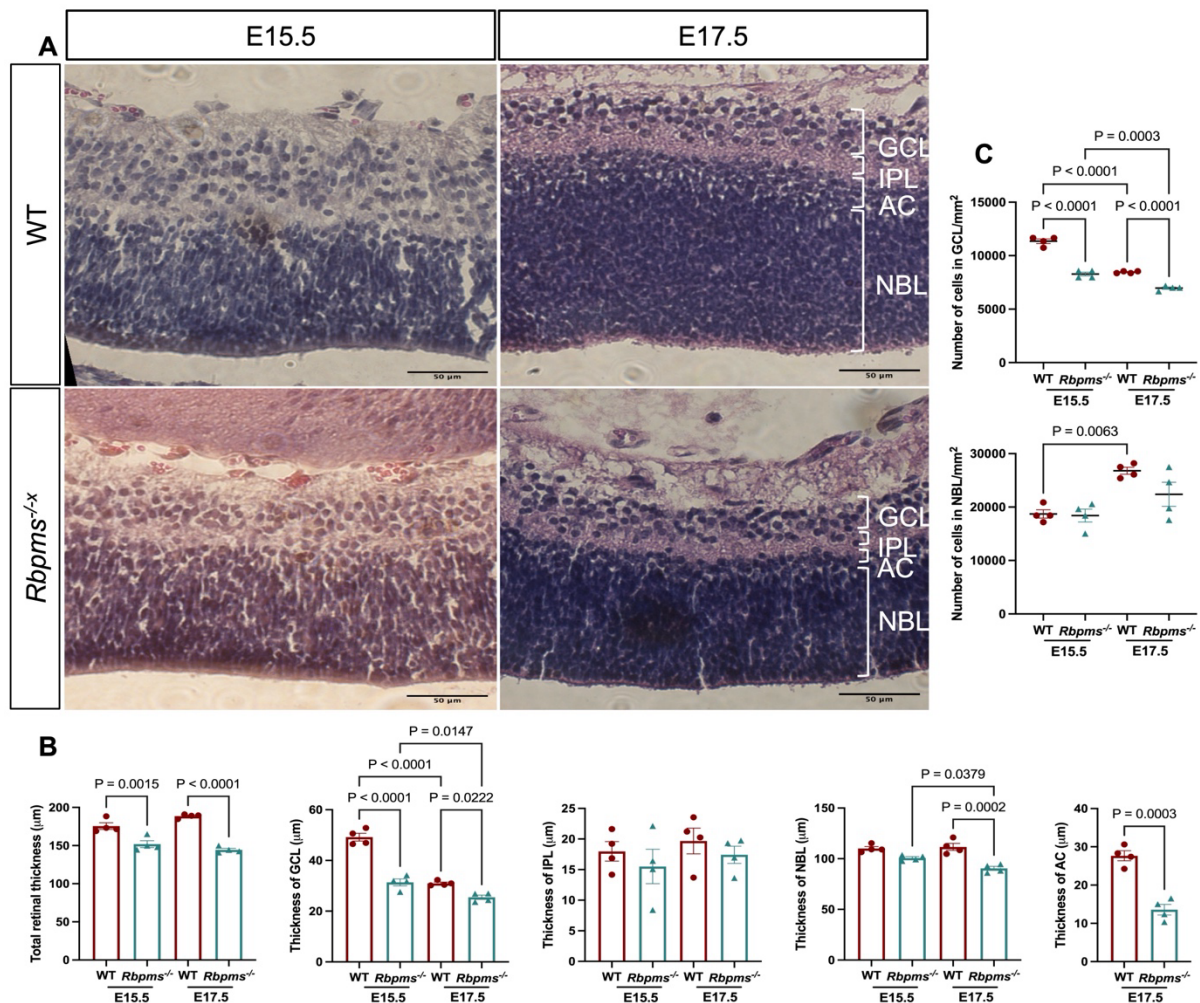


Figure 5 *Rbpms* deletion causes delayed development of embryonic retinal lamination patterns.

(A) Retinal cryosection of WT and *Rbpms*^{-/-} E15.5 and E17.5 retinas were H&E stained. Scale bars equal 50 µm. (B) Statistical analysis demonstrated that *Rbpms*^{-/-} retinas showed a notable reduction in the thickness of the total retinal layers, GCL, IPL, NBL, and AC, compared to the WT retinas. (C) Statistical analysis demonstrated that *Rbpms*^{-/-} retinas exhibited a significant decrease in the cell count in the GCL decreased significantly. At the same time, no variance was observed in the NBL compared to the WT retinas. n = 4 in each group. Error bars represent the mean ± SEM, and differences were evaluated through one-way ANOVA followed by Tukey's test for multiple comparisons or unpaired t-tests. NBL, neuroblastic cell layer; IPL, inner plexiform layer; AC, amacrine cells; GCL, ganglion cells layer.

5.6. *Rbpms* mutant retina RGC differentiation is significantly impeded.

During retinal development, RGCs in mice are the earliest type of neurons to be generated in the retina⁹. The reduction in the cell count within the GCL in the *Rbpms*^{-/-} retina may hinder

the lamination pattern of differentiation. To further characterize RGC differentiation within the GCL layer, we labeled the RGCs in WT and *Rbpms* mutant E15.5 retinas using Brn3a. In whole-mount confocal images, we observed that *Rbpms*^{-/-} retinas showed significantly lower Brn3a immunoreactivity than WT (Figure 6A). In cryosections, we observed that rounded, well-defined Brn3a⁺ RGCs were seen in WT, whereas only individual fusiform Brn3a⁺ RGCs were seen in *Rbpms* knockout retinas (Figure 6B). The earliest-born cells, the RGCs, extend a leading basal process through which the nucleus subsequently translocates⁵⁵. RGC migration to the GCL is necessary for the differentiation process. Observations revealed a clustering of Brn3a⁺ RGCs within the GCL (red arrows) in WT. Some Brn3a⁺ RGCs in the NBL layer showed radial extensions towards the retina's inner surface (white arrows). In contrast, Brn3a⁺ RGCs in the defective *Rbpms*^{-/-} retina remained below the GCL layer without migrating to the GCL layer (white arrows) (Figure 6A). Finally, a notable difference in Brn3a⁺ RGC density was observed between WT and *Rbpms*^{-/-} retinas. In this respect, the density of Brn3a⁺ RGC in *Rbpms*^{-/-} retinas was only $869.4 \pm 220.7/\text{mm}^2$, whereas the density of Brn3a⁺ RGC in WT was as high as $4073 \pm 162.9/\text{mm}^2$ ($P < 0.0001$) (Figure 6B).

RGCs are the sole type of neurons responsible for transmitting visual signals from the retina to the brain via the ON⁵⁶. WT and *Rbpms*^{-/-} ON sections were labeled using SMI-32 for neurofilament and GS-IB4 for vessels (Figure 6C). The results revealed a substantial reduction in the area fraction of SMI32 immunostaining within the ON of *Rbpms*-deficient embryos compared to WT embryos at E15.5 (Figure 6D).

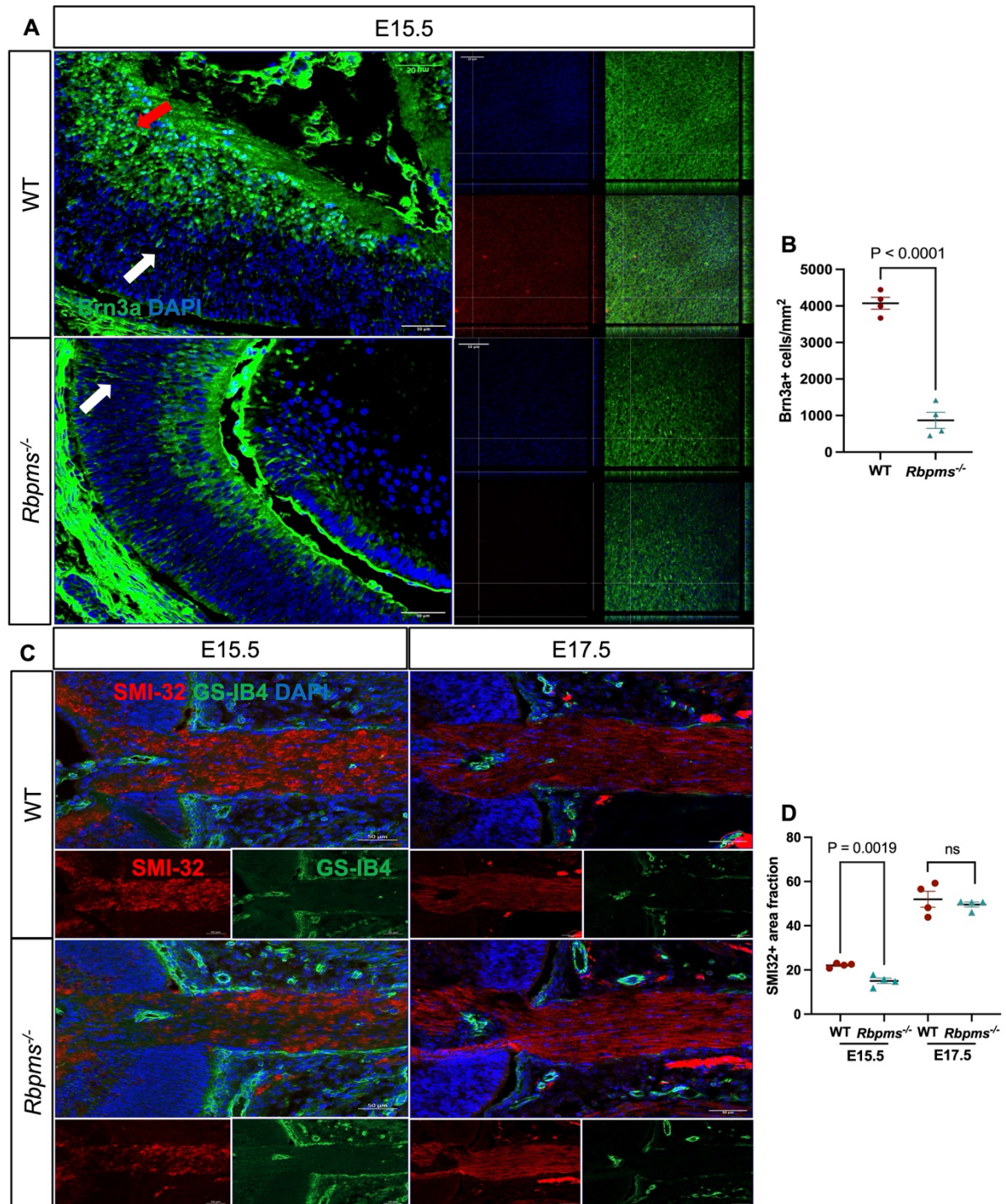


Figure 6 *Rbpms* mutant retina RGC differentiation is significantly impeded.

(A) Retinal cryosections of WT and *Rbpms*^{-/-} E15.5 embryos were immunolabeled with anti-Brn3a (green) and counterstained for nuclei using DAPI (blue). Scale bars indicate 50 μ m. The window on the right displays confocal images of the retinal flat mount of WT and *Rbpms*^{-/-} E15.5 embryos that were stained with anti-RBPMS (in red) and anti-Brn3a (in green), and then nuclei were stained with DAPI (blue). The scale bars represent 10 μ m. (B) Statistical analysis demonstrated that *Rbpms*^{-/-} retinas demonstrated a notable decline in the density of Brn3a+ cells in the cryosections. (C) ON cryosections of WT and *Rbpms*^{-/-} E15.5 and E17.5 embryos

were immunolabeled with SMI-32 (red), GS-IB4 (green), and counterstained for nuclei with DAPI (blue), with scale bars indicating 50 μm . (D) Statistical analysis demonstrated that *Rbpms*^{-/-} retinas exhibited a notable reduction in the area fraction of SMI-32 relative to the WT retinas. $n = 4$ in each group. Error bars represent the mean \pm SEM, and differences were evaluated through one-way ANOVA followed by Tukey's test for multiple comparisons or unpaired t-test.

5.7. RGCs fate specification is perturbed in the absence of *Rbpms*.

Since the number of RGCs in the GCL layer of *Rbpms*-deficient retinas was reduced while the number of nuclei in the NBL layer was unchanged, we speculated whether the fate of RPCs to specify RGCs was perturbed. We investigated PAX6 (a neural ectodermal cell fate determinant⁵⁷) expression in WT and *Rbpms* mutant E15.5 and E17.5 retinas (Figure 7A). The findings indicated a significant reduction in the density of PAX6+ cells in *Rbpms* mutant retinas (E15.5: $2544 \pm 190.5/\text{mm}^2$; E17.5: $1980 \pm 176.5/\text{mm}^2$) when compared to WT retinas (E15.5: $6070 \pm 444.9/\text{mm}^2$; E17.5: $3847 \pm 165.6/\text{mm}^2$) (Figure 7B).

TUJ1 antibodies bind to β -tubulin, a marker of early neurons that appears shortly following terminal mitosis^{58,59}. We observed TUJ1-labeled cells positioned along both boundaries of the IPL, as well as TUJ1+ neuroblasts in the NBL in both WT and *Rbpms*^{-/-} retinas at E15.5 and E17.5 (Figure 7C). However, no statistically significant changes in the TUJ1 positive area were observed at E15.5 or E17.5 (Figure 7D).

Microglia are essential for supporting neuronal survival and influencing neurogenesis during both developmental stages and in adult neurogenic zones^{60,61}. We observed Iba1+ macrophages distributed in the vitreous and Iba1+ microglia in the GCL (Figure 7E). Although the distribution of Iba1+ cells did not differ between WT and *Rbpms*^{-/-} retinas, the density of Iba1+ cells in the defective retina ($83.78 \pm 12.71/\text{mm}^2$) was significantly lower than in WT ($130.9 \pm 10.36/\text{mm}^2$) at E15.5 (Figure 7F). These data suggest that RGCs fate specification and differentiation are perturbed without *Rbpms*.

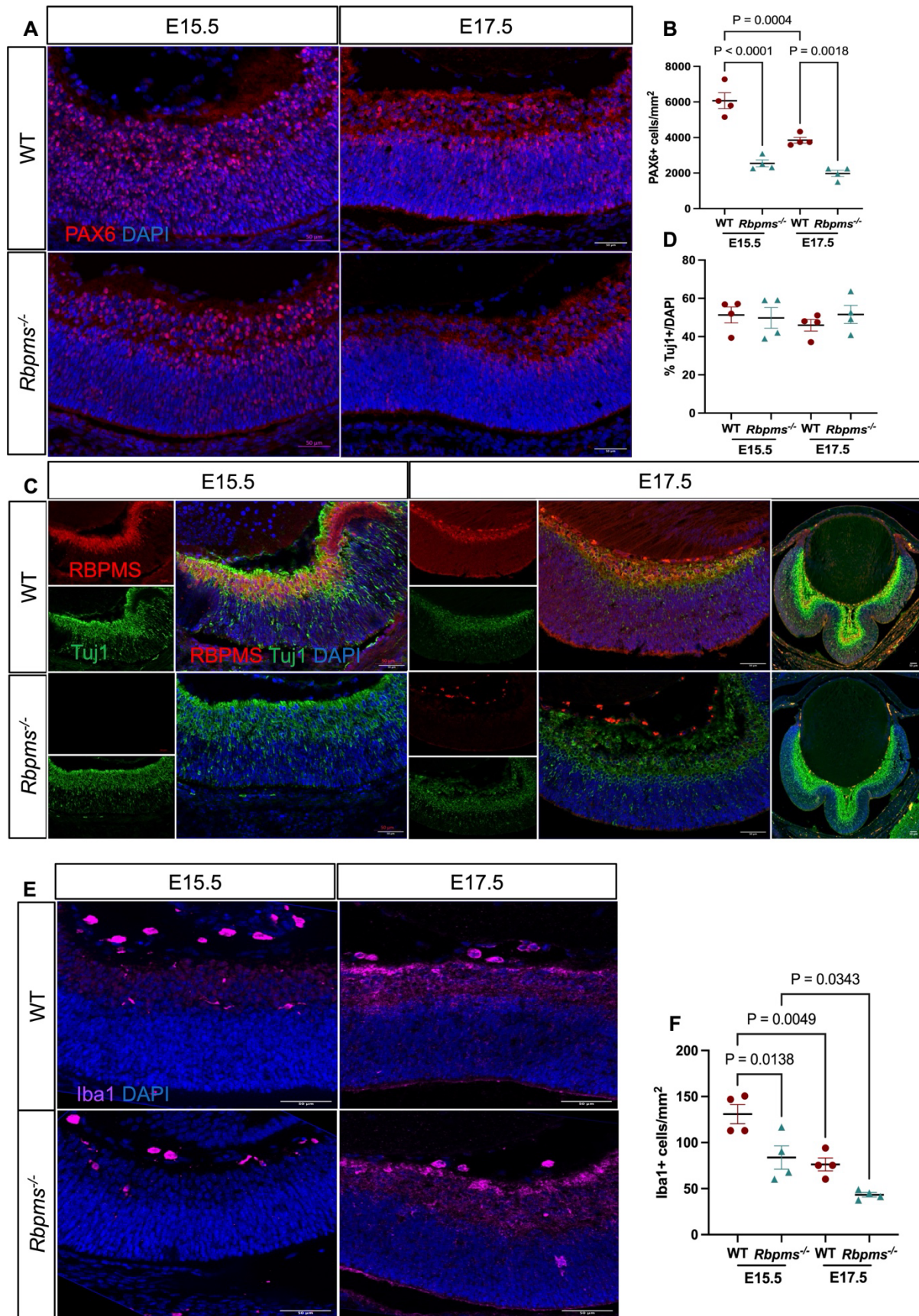


Figure 7 RGCs fate specification is perturbed in the absence of *Rbpms*.

(A) Retinal cryosections of WT and *Rbpms*^{-/-} E15.5 and E17.5 embryos were immunolabeled with anti-PAX6 (red), and nuclear was performed using DAPI (blue). Scale bars represent a length of 50 μm . (B) Statistical analysis demonstrated that *Rbpms*^{-/-} retinas exhibited a significant decrease in the PAX6 positive RGC density compared to the WT retinas. (C) Retinal cryosections from WT and *Rbpms*^{-/-} E15.5 and E17.5 embryos were stained with anti-RBPMS (red) and anti-TUJ1 (green) antibodies, with nuclear staining using DAPI (in blue). The far-right panels in (C) depict enlarged views of partial retina regions. Scale bars represent a length of 50 μm . (D) There were no statistically significant differences in the TUJ1 positive area observed in E15.5 and E17.5 retinas. (E) Retinal cryosections of WT and *Rbpms*^{-/-} E15.5 and E17.5 embryos were immunolabeled with anti-Iba1 (purple), with nuclear staining using DAPI (in blue). Scale bars equal 50 μm . (F) Statistical analysis demonstrated that *Rbpms*^{-/-} retinas exhibited a significant reduction in the Iba1+ cell density relative to the WT retinas at E15.5, whereas there were no differences at E17.5. $n = 4$ in each group. Error bars represent the mean \pm SEM, and differences were evaluated through one-way ANOVA followed by Tukey's test for multiple comparisons or unpaired t-test.

6. Discussion

This study suggests that in adult mice and human retinas, RBPMS is localized within the cytoplasm of RGCs and primarily functions in a decline in expression in response to aging and stress stimuli, with no apparent alteration in its spatial distribution. Perturbations in RGC fate specification in the absence of *Rbpms* underscore its potential contribution to guiding RPCs towards specific lineages and retinal layering during the development of the retina. The outcomes of this investigation yield significant insights into the multifaceted roles of *Rbpms* in retinal development, cellular fate specification, differentiation, aging, and stress responses.

Neurological function with age-related variability is well documented since neuronal loss was formerly considered a general feature of 'normal' aging²⁷⁻²⁹. Nowadays, immunohistochemical staining of molecular markers unique to RGCs serves as the main technique for evaluating RGC viability and analyzing *Rbpms* gene expression across all RGC variants^{62,63}. In the retina of mice, the densities of RBPMS-positive RGCs align closely with estimates derived from HRP-based retrograde tracing, varying between roughly 5000 cells/mm² in the central region to approximately 1500 cells/mm² in the periphery⁶⁴. Recent estimates derived from dye and retrograde cell labeling suggest that the overall density of RBPMS-positive cells may closely match, ranging from 2944 to 3817 cells/mm²^{65,66}. Brn3a has been demonstrated to label approximately 80% of the overall RGC population, omitting certain subtypes associated with disease, including those RGCs that express melanopsin^{5,39}. In the mouse and rat retina, Brn3a has been reported to be present in approximately 85% and 95% of RGCs, respectively^{36,65}.

Interestingly, RBPMS immunoreactive somatic cells outnumber Brn3a somatic cells by approximately 20%. Several other investigations have indicated that Brn3a is absent but expressed in a significant proportion of RGCs. For instance, more RGCs in mice and rats are labeled retrogradely with fluorescent dyes than those that express Brn3a^{39,67,68}. Finally, in the retinas of Thy1-CFP transgenic mice, more RBPMS cells, which may be RGCs, were present compared to cells containing strongly fluorescent CFP^{69,70}. These findings suggest that RBPMS might be expressed across the entire RGC population, encompassing dRGCs. Analogously, our observations noted that RBPMS+Brn3a- RGCs potentially exhibit a higher abundance than Brn3a+RBPMS- RGCs within the retinal tissue under baseline conditions in the control group.

However, aside from its role in transcriptional co-regulation, the majority of research attention has been directed toward its functions within the cytoplasm, particularly concerning mRNA stability⁷¹, intracellular transport⁴ and localization within cytoplasmic granule^{4,21,72}. Indeed, we have validated that the marker represents the co-staining of the nucleus (Brn3a) and the

cytoplasm (RBPMS) in mice RGCs. Localization of RBPMS immunoreactivity primarily occurs within the cytoplasm of somatic cells, indicating a correlation with post-transcriptional control of gene expression. This correspondence is noteworthy since proteins containing RRM motifs are involved in mRNA stability, processing, translation, and transport ^{1,73-75}. RBPMS2 mRNA ² and Hermes/RBPMS immunoreactivity ⁴ are expressed solely in RGCs, encompassing embryonic clawed frogs and axon terminals of developing retinas in *Xenopus* and zebrafish embryos.

Conversely, in adult mammals, RBPMS signals are largely limited to the soma of RGCs. These distinct expression patterns could arise from decreased RBPMS presence in the axons of mammalian RGCs following axon and synapse development or from RBPMS2's selective presence in RGC axons and nerve endings in the retinas of mammals. A study indicated that RBPMS expression extends to the inner nuclear layer (INL) of human retinal slices, with reduced expression observed in the soma of RGCs ⁴¹. However, we observed that RBPMS is to exhibit subcellular localization within the cytoplasm in RGCs.

Aging has been correlated with a decline in retinal neurons, accompanied by various age-related quantitative changes, including diminished areas of dendritic and axonal arbors, as well as decreased cell and synaptic density ⁷⁶. Our findings align with reports of decreased neuronal density in elderly mice and human retinas ^{76,77}. Notably, our study found for the first time that the loss of RBPMS+Brn3a-RGCs showed a cliff-like slope of decline, whereas the loss of Brn3a+RBPMS-RGCs was relatively flat, and RBPMS+RGCs appeared more sensitive to aging. In fact, RGC loss has an added layer of complexity in that its loss only sometimes occurs homogeneously in the retina. Studies have shown that RGC loss can be localized to specific areas of the retina in the early stages of injury, suggesting that some regional differences in RGC susceptibility exist ⁷⁸.

Interestingly, our findings indicate that the age-related decline in RBPMS+ RGCs results in peripheral alterations, with a more significant loss in the peripheral retina compared to the central retina. RGC death and degeneration of their axons in the ON are responsible for vision loss in various optic neuropathies, including glaucoma. Similar regional differences in RGC vulnerability also occur post-optic nerve crush (ONC) ⁷⁹. RGCs located in the retinal periphery were identified as the earliest RGCs susceptible to ONC damage. Sustained elevation of IOP results in more significant damage to RGCs in the peripheral regions than the central regions of the retina ⁸⁰, which probably explains why peripheral visual field defects occur in glaucoma before central defects. RBPMS might be involved in preserving the structural integrity of peripheral RGCs or modulating their susceptibility to degenerative processes.

Brn3a is downregulated following an increase in IOP⁸¹, while IP-RGC preferentially survives⁸². Similar to previous results, in our two mouse models of in vitro glaucoma, Brn3a+RGCs survived significantly more than RBPMS+RGCs in young mice post hydrostatic injury and in middle-aged mice post oxidative stress injury. In experimental glaucoma models, dysfunction of the RGC is an early phase of the disease relative to eventual cell death. The RBPMS is closely associated with the function and dysfunction of the RGC⁵. RBPMS serves as both a marker of cell viability and an early indicator for detecting RGC apoptosis in the explant model⁸³. Thus, the reduced density of RBPMS implies not only the deactivation of RGCs but also the presence of partial RGC dysfunction. The significant decrease in RBPMS expression under high hydrostatic pressure and oxidative stress implies its sensitivity to cellular stress conditions. When subjected to stressors, the notable loss of RBPMS in the peripheral retinal area suggests a region-specific vulnerability that may have implications for stress-induced retinal pathologies. In neurodegenerative diseases, alterations may occur in the expression and subcellular localization of RBPMS. RBPMS may be transported to the tip of retinal axons and its target mRNA cargo via motor proteins moving along the RGC axon's microtubules. RGC transportome is highly enriched for RBPs⁸⁴. Under hypoxia conditions, the transfer of RBPMS protein from RGC bodies to axons in granules⁴. However, our findings indicate that the spatial distribution of RBPMS remains stable following exposure to aging, high hydrostatic pressure, and oxidative stress. Nevertheless, RBPMS's expression within the cytoplasm of RGCs is diminished. RBPMS might involve intricate cellular processes contributing to its consumption, including mRNA stability, translation, or stress granule dynamics.

RBPMS also participates in controlling gene expression at the transcriptional stage. The interaction between RBPMS and Smad proteins is strengthened by TGF- β signaling, facilitating the nuclear translocation of Smad4⁸⁵. This facilitates the transcriptional activity of genes responsive to TGF- β ⁸⁵. The exact role of RBPMS within ganglion cells and retinal tissue is not fully understood. Nonetheless, its connection with Smad4, influencing TGF- β signaling pathways, suggests a possible involvement in the development and organization of retinal structures^{86,87}. Evidence supporting this is seen in the mouse retina, where Smad4 deficiency specifically disrupts RGC development and leads to misrouting of RGC axons toward the ON head⁸⁸. In single-cell RNA sequencing of retinal development, *Rbpms* was identified as a uniquely expressed gene found solely within the RGC and classified as associated with RGC differentiation²²⁻²⁵. ISH analysis on retinal sections from the African clawed toad (*Xenopus laevis*) indicated the first presence of Hermes mRNA in the central retina's GCL at stage 32, just after the initiation of RGC differentiation⁴. Immunostaining later confirmed the appearance of Hermes protein at stages 35/36⁴. Studies using cumulative labeling with BrdU injections

and rhodamine-dextran tracing in mice have shown that the first RGC appeared around embryonic days E11 to E12¹⁰. Immunostaining studies during retinogenesis in C57BL/6J mice showed no RBPMS detection in the retina at E11.5. By E12.5, however, cells positive for RBPMS began appearing centrally in the retina, expressing Brn3a, which marked the location of RGCs within the developing tissue⁸⁹. Our findings are consistent with previous findings that RBPMS was found to be expressed exclusively in RGCs and co-localized with Brn3a in both E15.5-17.5 retinas, suggesting that the commencement of RBPMS expression ought to be early in the process of RGC differentiation. RBPMS expression in RGCs during embryonic development indicates that it is potentially involved in directing neuronal development at an early stage.

The proliferation of RPCs is intricately linked to the specification of cell fates, thereby coordinating the generation of retinal cell types in accurate proportions and at the correct stages of development^{90,91}. RPC capabilities continuously change during retinogenesis as the external environment of retinal development changes^{91,92}. Sox2, PAX6, and Vsx2/Chx10, key transcription factors, are crucial in controlling the proliferation of pluripotent RPCs and regulating the expression of essential competence factors throughout the initial stages of retinal development⁹³. In mice, PAX6 is crucial in forming all retinal cell types except anaplastic cells⁹⁴. In early development, PAX6 stimulates the expression of Atoh7/Math5⁹⁵, while Atoh7 acts upstream of Pou4f1/Brn3a^{96,97}. In the absence of PAX6, the proliferation of RPCs is reduced⁹⁸. Brn3a orchestrates RGC differentiation, specification, and axon elongation^{97,99} and is also involved in neuronal survival by activating pro-survival genes and repressing pro-apoptotic genes¹⁰⁰. In our study, defects in *Rbpms* caused the absence of 79% Brn3a+cells and 58% PAX6+cells compared to the WT retina. The data demonstrate that *Rbpms* is crucial for RGC development, and its absence severely affects the differentiation process of RGC. In addition, microglia play a potential role in blood vessel formation, neuronal birth and survival, and synaptic refinement¹⁰¹. *Csf1r*^{-/-} microglia depletion in mice increases the developmental density of RGC subsets, and complement-mediated phagocytosis is involved in this process¹⁰². Our results indicate that besides the loss of RGCs, defects in *Rbpms* resulted in the loss of 36% of Iba1+cells and reduced SMI-32 immunoreactivity in the ON but did not affect the expression of TUJ1. TUJ1 is expressed in retinal cells beyond RGCs, and its expression correlates with cell-specific developmental programs¹⁰³. The data reveals that *Rbpms* is indispensable for retinal neuronal differentiation, influencing RPC proliferation and regulating RGC differentiation through transcription factors, which may play a crucial role in signaling events that regulate gene expression or direct the progenitor cells of the retina towards specific lineages.

A defining characteristic of the retina is its intricate, highly organized structure. Retinal cells must accurately position themselves to cover the entire retinal surface, while retinal neurons extend their processes and establish synaptic connections within distinct layers. There are no apparent abnormalities in the pattern of retinal lamination in Hermes-depleted zebrafish embryos⁴. Histological analysis using H&E on retinal sections from WT, *Rbpms* CreERT2/+, and *Rbpms* CreERT2/CreERT2 mice showed that the retinal structure remained unchanged, with no significant differences in cell counts within the GCL across the three groups⁸⁹. Our results also revealed that *Rbpms* deficiency did not affect the specification of retinal lamination patterns, which is consistent with previous findings. However, our data still demonstrate that at E17.5, AC, NBL, and GCL thickness, cell densities in the NBL and GCL are significantly lower in the absence of *Rbpms* than in the WT retinas. These results demonstrate that deletion of the *Rbpms* gene affects the course of embryonic retinal development.

Notably, as summarized by Hisato Kondoh, gene knockouts or mutations affecting retinal and lens development frequently lead to phenotypes such as microphthalmia, absent optic vesicles, anophthalmia, or retinal defects¹⁰⁴. Among these, only *Brn3b* deletion in mice has been demonstrated to specifically impair RGCs, with 70% of the RGC loss attributed to apoptosis in the mutant ganglion cells^{105,106}. Similarly, *Rbpms* knockout embryos show a significant disruption in RGC generation from RPCs, while overall eye development remains unaffected. Remarkably, the loss of Brn3a+ RGCs in these embryos is as high as 79%. Thus, the precise mechanism through which *Rbpms* selectively impacts RGC generation warrants further investigation. Previous studies on *Sey* mutant mice (a classic microphthalmia model) have revealed that *Pax6* mutations result in microphthalmia in heterozygous embryos and anophthalmia in homozygous embryos^{107,108}. This underscores the highly dose-sensitive nature of *Pax6* function during normal eye development. Our findings suggest that in the retinas of *Rbpms*^{-/-} embryos, PAX6 is not entirely inactivated, with 42% of PAX6+ cells remaining. This residual expression likely explains why *Rbpms* loss does not lead to gross ocular malformations.

RBPMS has been reported to bind to the 3' UTR of key Wnt-related mRNAs, including *Wnt3*, *Wnt8A*, and β -catenin, thereby facilitating their translation and ensuring proper mesoderm formation and cardiomyocyte differentiation¹⁸. The canonical Wnt/ β -catenin signaling pathway is essential for retinal development, contributing to key processes such as the establishment of the visual field, the formation of retinal and vitreous vasculature, and the maintenance of stem cells¹⁰⁹. Moreover, this pathway is essential for maintaining retinal progenitor cells during early development and injury-induced regeneration¹¹⁰. In addition to the canonical pathway, β -catenin-independent non-canonical Wnt signaling acts as a crucial regulator of proper

cellular development ¹¹¹. For instance, Wnt11 and Frizzled5 activation counteract β -catenin signaling, preventing the suppression of retinal identity in zebrafish while promoting uniformity in ocular region cells ¹¹². Furthermore, the loss of Wnt4 function has been linked to the depletion of Rx and Pax6 in frog eyes, mediated through EAF2 ¹¹³. RGCs have been identified as target cells of Wnt3a ¹¹⁴. In the ONC mouse model, intravitreal injection of exogenous Wnt3a has been shown to enhance axon regeneration and improve RGC survival ¹¹⁵. Likewise, in models of spinal cord injury, Wnt3a has been shown to stimulate neurite extension and promote neural stem cell differentiation into neurons at the injury site ¹¹⁶. Additionally, Musada et al. ¹¹⁴ demonstrated that recombinant Wnt5a delivery following optic nerve injury can promote axon regeneration and enhance RGC survival.

The loss of RBPMS has been shown to disrupt Wnt signaling ¹⁸. This disruption likely underlies the impaired differentiation of RGCs observed in *Rbpms* knockout embryos, making it reasonable to hypothesize that RGC-specific deficits may stem from altered Wnt signaling. Investigating how RBPMS regulates Wnt signaling during RGC differentiation could uncover the molecular mechanisms underlying retinal development and shed light on pathways that selectively affect RGCs without influencing other retinal cell types.

Wnt signaling's role in driving neuronal regeneration and differentiation, together with RBPMS's function in maintaining the retinal progenitor cell pool, positions the RBPMS /Wnt pathway as a promising therapeutic target for regulating retinal axon regeneration and promoting RGC survival. Future research should aim to clarify the molecular relationships between RBPMS and Wnt-associated mRNAs, including WNT3 and β -catenin, to deepen our understanding of its role in regulating retinal development. Concurrently, the development of drugs targeting the RBPMS/Wnt pathway could be explored, with animal models used to evaluate their effects on RGC survival and axon regeneration, potentially offering therapeutic strategies for glaucoma and retinal injuries.

Translational research efforts should aim to apply RBPMS/Wnt-targeted therapies in human retinal diseases and optic nerve injuries, with the goal of enhancing RGC survival and promoting axon regeneration through the modulation of Wnt signaling. Additionally, understanding the dose-sensitive effects of RBPMS and its interactions with Wnt signaling could form the basis for developing personalized treatments for retinal developmental disorders and neurodegenerative diseases. In-depth research into the RBPMS/Wnt pathway holds the potential to pave the way for novel therapeutic approaches to retinal and optic nerve-related diseases, accelerating the transition from basic research to clinical application.

6.1. Conclusion

In conclusion, this comprehensive study reveals the intricate involvement of *Rbpms* in various aspects of retinal development, RGC differentiation, aging, and stress responses. The findings collectively point to RBPMS as a multifunctional RNA-binding protein that plays a pivotal role in maintaining retinal homeostasis across different contexts. Understanding the precise mechanisms by which *Rbpms* exert its effects could potentially unveil novel therapeutic avenues for retinal disorders and shed light on broader RNA-related processes in neuronal systems. Further research is warranted to dissect the molecular pathways and interactions underlying *Rbpms*-mediated cellular processes, ultimately advancing our comprehension of retinal biology and associated pathologies.

6.2. Limitations of the project

Currently, this project still has certain limitations. Firstly, the molecular mechanisms of *Rbpms* in the process of RGC differentiation remain insufficiently understood, particularly regarding the regulatory networks and specific functions of its target genes. Secondly, current research primarily focuses on animal models, with insufficient validation of RBPMS expression patterns in the human retina and its potential therapeutic applications for retinal diseases. This gap introduces significant uncertainty regarding the feasibility of clinical translation. Additionally, there are currently no effective exogenous drugs available to regulate RBPMS, which limits its potential for development in therapeutic applications. Furthermore, studies on the dose-dependent effects of RBPMS and its roles across various retinal cell types remain limited, hindering a comprehensive understanding of its potential as a therapeutic target. Therefore, more in-depth and systematic research addressing these issues is needed in the future to facilitate the effective translation of this project from basic research to clinical applications.

7. REFERENCES

1. Lunde BM, Moore C, Varani G. RNA-binding proteins: modular design for efficient function. *Nature reviews Molecular cell biology* 2007; **8**(6): 479-90.
2. Gerber WV, Yatskievych TA, Antin PB, Correia KM, Conlon RA, Krieg PA. The RNA-binding protein gene, hermes, is expressed at high levels in the developing heart. *Mechanisms of Development* 1999; **80**(1): 77-86.
3. Piri N, Kwong JM, Song M, Caprioli J. Expression of hermes gene is restricted to the ganglion cells in the retina. *Neuroscience letters* 2006; **405**(1-2): 40-5.
4. Hörnberg H, Wollerton-van Horck F, Maurus D, et al. RNA-binding protein Hermes/RBPMS inversely affects synapse density and axon arbor formation in retinal ganglion cells in vivo. *Journal of Neuroscience* 2013; **33**(25): 10384-95.
5. Rodriguez AR, de Sevilla Müller LP, Brecha NC. The RNA binding protein RBPMS is a selective marker of ganglion cells in the mammalian retina. *J Comp Neurol* 2014; **522**(6): 1411-43.
6. Kwong JMK, Caprioli J, Piri N. RNA Binding Protein with Multiple Splicing: A New Marker for Retinal Ganglion Cells. *Investigative Ophthalmology & Visual Science* 2010; **51**(2): 1052-8.
7. la Vail MM, Rapaport DH, Rakic P. Cytogenesis in the monkey retina. *Journal of Comparative Neurology* 1991; **309**(1): 86-114.
8. Turner DL, Cepko CL. A common progenitor for neurons and glia persists in rat retina late in development. *Nature* 1987; **328**(6126): 131-6.
9. Whitney IE, Butrus S, Dyer MA, Rieke F, Sanes JR, Shekhar K. Vision-Dependent and -Independent Molecular Maturation of Mouse Retinal Ganglion Cells. *Neuroscience* 2023; **508**: 153-73.
10. Dräger UC. Birth dates of retinal ganglion cells giving rise to the crossed and uncrossed optic projections in the mouse. *Proceedings of the Royal society of London Series B Biological sciences* 1985; **224**(1234): 57-77.
11. Farah MH, Easter Jr SS. Cell birth and death in the mouse retinal ganglion cell layer. *Journal of Comparative Neurology* 2005; **489**(1): 120-34.
12. Voinescu PE, Kay JN, Sanes JR. Birthdays of retinal amacrine cell subtypes are systematically related to their molecular identity and soma position. *Journal of Comparative Neurology* 2009; **517**(5): 737-50.
13. Martersteck EM, Hirokawa KE, Evarts M, et al. Diverse central projection patterns of retinal ganglion cells. *Cell reports* 2017; **18**(8): 2058-72.
14. Hu M, Easter Jr SS. Retinal neurogenesis: the formation of the initial central patch of postmitotic cells. *Developmental biology* 1999; **207**(2): 309-21.

15. Holt CE, Bertsch TW, Ellis HM, Harris WA. Cellular determination in the *Xenopus* retina is independent of lineage and birth date. *Neuron* 1988; **1**(1): 15-26.
16. Prada C, Puga J, Pérez-Méndez L, López R, Ramírez G. Spatial and temporal patterns of neurogenesis in the chick retina. *European Journal of Neuroscience* 1991; **3**(6): 559-69.
17. Hoshino A, Ratnapriya R, Brooks MJ, et al. Molecular anatomy of the developing human retina. *Developmental cell* 2017; **43**(6): 763-79. e4.
18. Bartsch D, Kalamkar K, Ahuja G, et al. mRNA translational specialization by RBPMS presets the competence for cardiac commitment in hESCs. *Sci Adv* 2023; **9**(13): eade1792.
19. Holt CE, Schuman EM. The central dogma decentralized: new perspectives on RNA function and local translation in neurons. *Neuron* 2013; **80**(3): 648-57.
20. Prashad S, Gopal PP. RNA-binding proteins in neurological development and disease. *RNA biology* 2021; **18**(7): 972-87.
21. Furukawa MT, Sakamoto H, Inoue K. Interaction and colocalization of HERMES/RBPMS with NonO, PSF, and G3BP1 in neuronal cytoplasmic RNP granules in mouse retinal line cells. *Genes to Cells* 2015; **20**(4): 257-66.
22. Clark BS, Stein-O'Brien GL, Shiao F, et al. Single-Cell RNA-Seq Analysis of Retinal Development Identifies NFI Factors as Regulating Mitotic Exit and Late-Born Cell Specification. *Neuron* 2019; **102**(6): 1111-26.e5.
23. Brodie-Kommit J, Clark BS, Shi Q, et al. Atoh7-independent specification of retinal ganglion cell identity. *Science Advances* 2021; **7**(11): eabe4983.
24. Shekhar K, Whitney IE, Butrus S, Peng Y-R, Sanes JR. Diversification of multipotential postmitotic mouse retinal ganglion cell precursors into discrete types. *eLife* 2022; **11**: e73809.
25. Teotia P, Niu M, Ahmad I. Mapping developmental trajectories and subtype diversity of normal and glaucomatous human retinal ganglion cells by single-cell transcriptome analysis. *STEM CELLS* 2020; **38**(10): 1279-91.
26. Diez-Roux G, Banfi S, Sultan M, et al. A high-resolution anatomical atlas of the transcriptome in the mouse embryo. *PLoS biology* 2011; **9**(1): e1000582.
27. Miller A, Alston R, Mountjoy C, CORSELLIS J. Automated differential cell counting on a sector of the normal human hippocampus: the influence of age. *Neuropathology and applied neurobiology* 1984; **10**(2): 123-41.
28. Swaab DF, Fliers E, Partiman T. The suprachiasmatic nucleus of the human brain in relation to sex, age and senile dementia. *Brain research* 1985; **342**(1): 37-44.

29. Terry RD, DeTeresa R, Hansen LA. Neocortical cell counts in normal human adult aging. *Annals of Neurology: Official Journal of the American Neurological Association and the Child Neurology Society* 1987; **21**(6): 530-9.
30. Moons L, De Groef L. Multimodal retinal imaging to detect and understand Alzheimer's and Parkinson's disease. *Current opinion in neurobiology* 2022; **72**: 1-7.
31. Christinaki E, Kulenovic H, Hadoux X, et al. Retinal imaging biomarkers of neurodegenerative diseases. *Clinical and Experimental Optometry* 2022; **105**(2): 194-204.
32. La Morgia C, Di Vito L, Carelli V, Carbonelli M. Patterns of retinal ganglion cell damage in neurodegenerative disorders: parvocellular vs magnocellular degeneration in optical coherence tomography studies. *Frontiers in neurology* 2017; **8**: 710.
33. Levin LA, Gordon LK. Retinal ganglion cell disorders: types and treatments. *Progress in Retinal and Eye Research* 2002; **21**(5): 465-84.
34. Kwong JM, Quan A, Kyung H, Piri N, Caprioli J. Quantitative analysis of retinal ganglion cell survival with Rbpms immunolabeling in animal models of optic neuropathies. *Investigative ophthalmology & visual science* 2011; **52**(13): 9694-702.
35. Sargoy A, Sun X, Barnes S, Brecha NC. Differential calcium signaling mediated by voltage-gated calcium channels in rat retinal ganglion cells and their unmyelinated axons. *PloS one* 2014; **9**(1): e84507.
36. Nadal-Nicolás FM, Jiménez-López M, Sobrado-Calvo P, et al. Brn3a as a marker of retinal ganglion cells: qualitative and quantitative time course studies in naive and optic nerve-injured retinas. *Invest Ophthalmol Vis Sci* 2009; **50**(8): 3860-8.
37. Sanchez-Migallon MC, Valiente-Soriano FJ, Nadal-Nicolas FM, Vidal-Sanz M, Agudo-Barriuso M. Apoptotic Retinal Ganglion Cell Death After Optic Nerve Transection or Crush in Mice: Delayed RGC Loss With BDNF or a Caspase 3 Inhibitor. *Invest Ophthalmol Vis Sci* 2016; **57**(1): 81-93.
38. Chen SK, Badea TC, Hattar S. Photoentrainment and pupillary light reflex are mediated by distinct populations of ipRGCs. *Nature* 2011; **476**(7358): 92-5.
39. Nadal-Nicolas FM, Jimenez-Lopez M, Salinas-Navarro M, et al. Whole number, distribution and co-expression of brn3 transcription factors in retinal ganglion cells of adult albino and pigmented rats. *PLoS One* 2012; **7**(11): e49830.
40. Nadal-Nicolás FM, Galindo-Romero C, Lucas-Ruiz F, et al. Pan-retinal ganglion cell markers in mice, rats, and rhesus macaques. *Zool Res* 2023; **44**(1): 226-48.
41. Pereiro X, Ruzafa N, Urcola JH, Sharma SC, Vecino E. Differential Distribution of RBPMS in Pig, Rat, and Human Retina after Damage. *International Journal of Molecular Sciences* 2020; **21**(23): 9330.

42. Loya CM, Van Vactor D, Fulga TA. Understanding neuronal connectivity through the post-transcriptional toolkit. *Genes & development* 2010; **24**(7): 625-35.
43. Chan JW, Chan NCY, Sadun AA. Glaucoma as Neurodegeneration in the Brain. *Eye Brain* 2021; **13**: 21-8.
44. Osborne N, Ugarte M, Chao M, et al. Neuroprotection in relation to retinal ischemia and relevance to glaucoma. *Survey of ophthalmology* 1999; **43**: S102-S28.
45. Quigley HA, Broman AT. The number of people with glaucoma worldwide in 2010 and 2020. *The British journal of ophthalmology* 2006; **90**(3): 262.
46. Weinreb RN, Aung T, Medeiros FA. The pathophysiology and treatment of glaucoma: a review. *Jama* 2014; **311**(18): 1901-11.
47. Tan NY, Sng CC, Jonas JB, Wong TY, Jansonius NM, Ang M. Glaucoma in myopia: diagnostic dilemmas. *British Journal of Ophthalmology* 2019.
48. Shestopalov VI, Spurlock M, Gramlich OW, Kuehn MH. Immune Responses in the Glaucomatous Retina: Regulation and Dynamics. *Cells* 2021; **10**(8).
49. Dutta S, Sengupta P. Men and mice: Relating their ages. *Life Sci* 2016; **152**: 244-8.
50. Flurkey K, Harrison D. The mouse in aging research. Burlington: American College Laboratory Animal Medicine. Elsevier Amsterdam; 2007.
51. Bell BA, Kaul C, Bonilha VL, Rayborn ME, Shadrach K, Hollyfield JG. The BALB/c mouse: Effect of standard vivarium lighting on retinal pathology during aging. *Experimental Eye Research* 2015; **135**: 192-205.
52. Hermenean A, Trotta MC, Gharbia S, et al. Changes in Retinal Structure and Ultrastructure in the Aged Mice Correlate With Differences in the Expression of Selected Retinal miRNAs. *Front Pharmacol* 2020; **11**: 593514.
53. Chu VT, Weber T, Graf R, et al. Efficient generation of Rosa26 knock-in mice using CRISPR/Cas9 in C57BL/6 zygotes. *BMC Biotechnol* 2016; **16**: 4.
54. Tröder SE, Ebert LK, Butt L, Assenmacher S, Schermer B, Zevnik B. An optimized electroporation approach for efficient CRISPR/Cas9 genome editing in murine zygotes. *PLoS One* 2018; **13**(5): e0196891.
55. McLoon SC, Barnes R. Early differentiation of retinal ganglion cells: an axonal protein expressed by premigratory and migrating retinal ganglion cells. *Journal of Neuroscience* 1989; **9**(4): 1424-32.
56. Mead B, Tomarev S. Evaluating retinal ganglion cell loss and dysfunction. *Exp Eye Res* 2016; **151**: 96-106.
57. Zhang X, Huang CT, Chen J, et al. Pax6 is a human neuroectoderm cell fate determinant. *Cell Stem Cell* 2010; **7**(1): 90-100.
58. Easter S, Ross LS, Frankfurter A. Initial tract formation in the mouse

- brain. *Journal of Neuroscience* 1993; **13**(1): 285-99.
59. Martinez-Morales J-R, Del Bene F, Nica G, Hammerschmidt M, Bovolenta P, Wittbrodt J. Differentiation of the Vertebrate Retina Is Coordinated by an FGF Signaling Center. *Developmental Cell* 2005; **8**(4): 565-74.
60. Ekdahl CT, Kokaia Z, Lindvall O. Brain inflammation and adult neurogenesis: the dual role of microglia. *Neuroscience* 2009; **158**(3): 1021-9.
61. Sato K. Effects of Microglia on Neurogenesis. *Glia* 2015; **63**(8): 1394-405.
62. Rheume BA, Jereen A, Bolisetty M, et al. Single cell transcriptome profiling of retinal ganglion cells identifies cellular subtypes. *Nature communications* 2018; **9**(1): 1-17.
63. Tran NM, Shekhar K, Whitney IE, et al. Single-cell profiles of retinal ganglion cells differing in resilience to injury reveal neuroprotective genes. *Neuron* 2019; **104**(6): 1039-55. e12.
64. Dräger UC, Olsen JF. Origins of crossed and uncrossed retinal projections in pigmented and albino mice. *Journal of Comparative Neurology* 1980; **191**(3): 383-412.
65. Galindo-Romero C, Aviles-Trigueros M, Jimenez-Lopez M, et al. Axotomy-induced retinal ganglion cell death in adult mice: quantitative and topographic time course analyses. *Experimental eye research* 2011; **92**(5): 377-87.
66. Pang J-J, Wu SM. Morphology and immunoreactivity of retrogradely double-labeled ganglion cells in the mouse retina. *Investigative Ophthalmology & Visual Science* 2011; **52**(7): 4886-96.
67. Quina LA, Pak W, Lanier J, et al. Brn3a-expressing retinal ganglion cells project specifically to thalamocortical and collicular visual pathways. *Journal of Neuroscience* 2005; **25**(50): 11595-604.
68. Jain V, Ravindran E, Dhingra NK. Differential expression of Brn3 transcription factors in intrinsically photosensitive retinal ganglion cells in mouse. *Journal of Comparative Neurology* 2012; **520**(4): 742-55.
69. Feng G, Mellor RH, Bernstein M, et al. Imaging neuronal subsets in transgenic mice expressing multiple spectral variants of GFP. *Neuron* 2000; **28**(1): 41-51.
70. Raymond ID, Vila A, Huynh U-CN, Brecha NC. Cyan fluorescent protein expression in ganglion and amacrine cells in a thy1-CFP transgenic mouse retina. *Molecular vision* 2008; **14**: 1559.
71. Rambout X, Detiffe C, Bruyr J, et al. The transcription factor ERG recruits CCR4–NOT to control mRNA decay and mitotic progression. *Nature Structural & Molecular Biology* 2016; **23**(7): 663-72.
72. Farazi TA, Leonhardt CS, Mukherjee N, et al. Identification of the RNA recognition element of the RBPMS family of RNA-binding proteins and their transcriptome-wide mRNA targets. *Rna* 2014; **20**(7): 1090-102.

73. Burd CG, Dreyfuss G. Conserved structures and diversity of functions of RNA-binding proteins. *Science* 1994; **265**(5172): 615-21.
74. Shimamoto A, Kitao S, Ichikawa K, et al. A unique human gene that spans over 230 kb in the human chromosome 8p11-12 and codes multiple family proteins sharing RNA-binding motifs. *Proc Natl Acad Sci U S A* 1996; **93**(20): 10913-7.
75. Maris C, Dominguez C, Allain FH. The RNA recognition motif, a plastic RNA-binding platform to regulate post-transcriptional gene expression. *Febs j* 2005; **272**(9): 2118-31.
76. Samuel MA, Zhang Y, Meister M, Sanes JR. Age-related alterations in neurons of the mouse retina. *J Neurosci* 2011; **31**(44): 16033-44.
77. Aggarwal P, Nag T, Wadhwa S. Age-related decrease in rod bipolar cell density of the human retina: an immunohistochemical study. *Journal of biosciences* 2007; **32**(2): 293-8.
78. Tapia ML, Nascimento-dos-Santos G, Park KK. Subtype-specific survival and regeneration of retinal ganglion cells in response to injury. *Frontiers in Cell and Developmental Biology* 2022; **10**.
79. Kingston R, Amin D, Misra S, Gross JM, Kuwajima T. Serotonin transporter-mediated molecular axis regulates regional retinal ganglion cell vulnerability and axon regeneration after nerve injury. *PLoS genetics* 2021; **17**(11): e1009885.
80. Mukai R, Park DH, Okunuki Y, et al. Mouse model of ocular hypertension with retinal ganglion cell degeneration. *PLoS One* 2019; **14**(1): e0208713.
81. Guo Y, Johnson E, Cepurna W, Jia L, Dyck J, Morrison JC. Does elevated intraocular pressure reduce retinal TRKB-mediated survival signaling in experimental glaucoma? *Experimental eye research* 2009; **89**(6): 921-33.
82. Pérez de Sevilla Müller L, Sargoy A, Rodriguez AR, Brecha NC. Melanopsin ganglion cells are the most resistant retinal ganglion cell type to axonal injury in the rat retina. *PLoS One* 2014; **9**(3): e93274.
83. Pattamatta U, McPherson Z, White A. A mouse retinal explant model for use in studying neuroprotection in glaucoma. *Experimental Eye Research* 2016; **151**: 38-44.
84. Schiapparelli LM, Shah SH, Ma Y, et al. The Retinal Ganglion Cell Transportome Identifies Proteins Transported to Axons and Presynaptic Compartments in the Visual System In Vivo. *Cell Rep* 2019; **28**(7): 1935-47.e5.
85. Sun Y, Ding L, Zhang H, et al. Potentiation of Smad-mediated transcriptional activation by the RNA-binding protein RBPMS. *Nucleic Acids Res* 2006; **34**(21): 6314-26.
86. Duenker N. Transforming growth factor-beta (TGF-beta) and programmed cell death in the vertebrate retina. *Int Rev Cytol* 2005; **245**: 17-43.

87. Wordinger RJ, Clark AF. Bone morphogenetic proteins and their receptors in the eye. *Exp Biol Med (Maywood)* 2007; **232**(8): 979-92.
88. Murali D, Kawaguchi-Niida M, Deng CX, Furuta Y. Smad4 is required predominantly in the developmental processes dependent on the BMP branch of the TGF- β signaling system in the embryonic mouse retina. *Invest Ophthalmol Vis Sci* 2011; **52**(6): 2930-7.
89. Guo L, Xie X, Wang J, et al. Inducible Rbpms-CreERT2 Mouse Line for Studying Gene Function in Retinal Ganglion Cell Physiology and Disease. *Cells* 2023; **12**(15): 1951.
90. Dyer MA, Cepko CL. p27^{Kip1} and p57^{Kip2} Regulate Proliferation in Distinct Retinal Progenitor Cell Populations. *The Journal of Neuroscience* 2001; **21**(12): 4259-71.
91. Livesey FJ, Cepko CL. Vertebrate neural cell-fate determination: Lessons from the retina. *Nature Reviews Neuroscience* 2001; **2**(2): 109-18.
92. Agathocleous M, Harris WA. From progenitors to differentiated cells in the vertebrate retina. *Annual Review of Cell and Developmental* 2009; **25**: 45-69.
93. Oliveira-Valença VM, Bosco A, Vetter ML, Silveira MS. On the Generation and Regeneration of Retinal Ganglion Cells. *Frontiers in Cell and Developmental Biology* 2020; **8**.
94. Marquardt T, Ashery-Padan R, Andrejewski N, Scardigli R, Guillemot F, Gruss P. Pax6 is required for the multipotent state of retinal progenitor cells. *Cell* 2001; **105**(1): 43-55.
95. Riesenber AN, Le TT, Willardsen MI, Blackburn DC, Vetter ML, Brown NL. Pax6 regulation of Math5 during mouse retinal neurogenesis. *Genesis* 2009; **47**(3): 175-87.
96. Liu W, Mo Z, Xiang M. The Ath5 proneural genes function upstream of Brn3 POU domain transcription factor genes to promote retinal ganglion cell development. *Proceedings of the National Academy of Sciences* 2001; **98**(4): 1649-54.
97. Pan L, Yang Z, Feng L, Gan L. Functional equivalence of Brn3 POU-domain transcription factors in mouse retinal neurogenesis. *Development* 2005; **132**(4): 703-12.
98. Philips GT, Stair CN, Young Lee H, et al. Precocious retinal neurons: Pax6 controls timing of differentiation and determination of cell type. *Dev Biol* 2005; **279**(2): 308-21.
99. Parmhans N, Fuller AD, Nguyen E, et al. Identification of retinal ganglion cell types and brain nuclei expressing the transcription factor Brn3c/Pou4f3 using a Cre recombinase knock-in allele. *J Comp Neurol* 2021; **529**(8): 1926-53.
100. Serrano-Saiz E, Leyva-Diaz E, De La Cruz E, Hobert O. BRN3-type POU Homeobox Genes Maintain the Identity of Mature Postmitotic Neurons in Nematodes and Mice. *Curr Biol* 2018; **28**(17): 2813-23 e2.

101. Li F, Jiang D, Samuel MA. Microglia in the developing retina. *Neural Development* 2019; **14**(1): 12.
102. Anderson SR, Roberts JM, Zhang J, et al. Developmental apoptosis promotes a disease-related gene signature and independence from CSF1R signaling in retinal microglia. *Cell reports* 2019; **27**(7): 2002-13. e5.
103. Sharma RK, Netland PA. Early born lineage of retinal neurons express class III β -tubulin isotype. *Brain Research* 2007; **1176**: 11-7.
104. Kondoh H. 21 - Development of the Eye. In: Rossant J, Tam PPL, eds. *Mouse Development*. San Diego: Academic Press; 2002: 519-38.
105. Gan L, Xiang M, Zhou L, Wagner DS, Klein WH, Nathans J. POU domain factor Brn-3b is required for the development of a large set of retinal ganglion cells. *Proceedings of the National Academy of Sciences* 1996; **93**(9): 3920-5.
106. Gan L, Wang SW, Huang Z, Klein WH. POU domain factor Brn-3b is essential for retinal ganglion cell differentiation and survival but not for initial cell fate specification. *Developmental biology* 1999; **210**(2): 469-80.
107. Hill RE, Favor J, Hogan BL, et al. Mouse small eye results from mutations in a paired-like homeobox-containing gene. *Nature* 1991; **354**(6354): 522-5.
108. Hogan BL, Horsburgh G, Cohen J, Hetherington CM, Fisher G, Lyon MF. Small eyes (Sey): a homozygous lethal mutation on chromosome 2 which affects the differentiation of both lens and nasal placodes in the mouse. *Development* 1986; **97**(1): 95-110.
109. Fujimura N. WNT/ β -catenin signaling in vertebrate eye development. *Frontiers in cell and developmental biology* 2016; **4**: 138.
110. Meyers JR, Hu L, Moses A, Kaboli K, Papandrea A, Raymond PA. β -catenin/Wnt signaling controls progenitor fate in the developing and regenerating zebrafish retina. *Neural Development* 2012; **7**(1): 30.
111. Shah R, Amador C, Chun ST, et al. Non-canonical Wnt signaling in the eye. *Progress in Retinal and Eye Research* 2023; **95**: 101149.
112. Cavodeassi F, Carreira-Barbosa F, Young RM, et al. Early stages of zebrafish eye formation require the coordinated activity of Wnt11, Fz5, and the Wnt/ β -catenin pathway. *Neuron* 2005; **47**(1): 43-56.
113. Maurus D, Heligon C, Bürger-Schwärzler A, Brändli AW, Kühl M. Noncanonical Wnt-4 signaling and EAF2 are required for eye development in *Xenopus laevis*. *The EMBO journal* 2005; **24**(6): 1181-91.
114. Musada GR, Dvorientchikova G, Myer C, Ivanov D, Bhattacharya SK, Hackam AS. The effect of extrinsic Wnt/ β -catenin signaling in Muller glia on retinal ganglion cell neurite growth. *Developmental Neurobiology* 2020; **80**(3-4): 98-110.
115. Patel AK, Park KK, Hackam AS. Wnt signaling promotes axonal regeneration following optic nerve injury in the mouse. *Neuroscience* 2017; **343**: 372-83.

116. Yin ZS, Zu B, Chang J, Zhang H. Repair effect of Wnt3a protein on the contused adult rat spinal cord. *Neurol Res* 2008; **30**(5): 480-6.

8. APPENDIX

8.1. List of figures

Figure 1 Variation of RBPMS in response to aging in the retinal flat mounts of <i>C57BL/6J</i> mice.....	21
Figure 2 RBPMS expression decreases under elevated hydrostatic pressure and oxidative stress.....	24
Figure 3 Characteristics and spatial distribution of structural features of <i>Rbpms</i> in age-related retinal neurodegeneration.....	27
Figure 4 RBPMS expression within the GCL of the developing retina.....	29
Figure 5 <i>Rbpms</i> deletion causes delayed development of embryonic retinal lamination patterns.....	31
Figure 6 <i>Rbpms</i> mutant retina RGC differentiation is significantly impeded.....	33
Figure 7 RGCs fate specification is perturbed in the absence of <i>Rbpms</i>	35

8.2. List of tables

Table 1 of primers used:.....	16
Table 2 Antibodies used for histological analyses.....	18
Table 3 The density of different types of RGCs in various regions of the retina throughout aging and neurodegeneration	25